A Novel p38 MAP kinase inhibitor and its pharmaceutically acceptable salts

1 Introduction

Inflammatory response is a basic protective immune process of an organism and is accompanied by symptoms such as redness, heat, swelling, and pain [1]. This is one of the mechanisms by which our body defends us from exogenous pathogens such as parasites, bacteria, viruses, and other harmful microorganisms. Diseases induced by chronic inflammation such as gastritis, colitis, dermatitis, rheumatoid arthritis, pulmonary diseases and type II diabetes etc. damage millions of people's health every year. Lately, there has been an increase in prevalence of these chronic inflammatory diseases. Furthermore, recent studies has provided evidence that inflammation is a critical initiation factor for several major diseases such as cancer, atherosclerosis, Alzheimer's disease, cardiovascular disease, neurological disorders, and pulmonary diseases [2–7]. Therefore, a better understanding of inflammation is clinically significant and could improve treatment strategies.

Various intracellular proteins can initiate inflammation.p38 proteins are a class of mitogen-activated protein kinases (MAPKs) that are major players during inflammatory responses, especially in macrophages. p38, also called cytokinin-specific binding protein (CSBP), was identified in1994 and is the mammalian ortholog of the yeast Hog1p MAP kinase [8]. p38 was isolated as a 38 kDa protein that is rapidly phosphorylated at a tyrosine residue in response to LPS stimulation, and the p38 gene has been cloned through binding of the p38 protein with pyridinyl imidazole derivatives [9]. Upregulation of p38 expression occurs in response to inflammatory and stress stimuli, such as cytokines, ultraviolet irradiation,osmotic and heat shock, and is involved in autophagy, apoptosis, and cell differentiation [10–14]. Evidence accrued from

scientific studies suggests that p38 plays an important role in arthritis and inflammation of the liver, kidney, brain, and lung and that it acts as a critical player in inflammatory diseases mediated by macrophages [15–17].

2 Structure, Function and mechanism of action of p38 Kinases

2.1 The p38 Family

The p38 family members are classified into four subtypes: α (MAPK14), β (MAPK11), γ (MAPK12/ERK6),andδ (MAPK13/SAPK4) (Table 1) [18].

Table 1: The p38 family

Table 1: p38 family members and their functions in inflammatory responses.

p38 isoform (molecular weight, kDa)	Distribution in tissue	Expressing cells	Inflammatory responses
p38 α	Ubiquitous	Macrophages, neutrophils	Cytokine production (IL-1 β, TNF- α, and IL-6); regulation of enzymes (iNOS, COX-2); involvement of cell proliferation and differentiation; induction of cardiomyocyte apoptosis.
p38 β	Ubiquitous	Endothelial cells, T cells	Regulation of cell differentiation; induction of cardiomyocyte hypertrophy.
p38 γ	Skeletal muscle	Not detected	Muscle differentiation.
p38 δ	Lung, kidney, testis, pancreas, and small	T cells, endothelial cells, and	Developmentally regulated; involvement of cell differentiation.

	intestine	macrophages	

Genes encoding p38α and p38β show 74% sequence homology, whereas γ and δ are more distant relatives, with approximately 62% sequence identity [19–20]. Genes encoding p38α and p38β are ubiquitously expressed within tissues, and especially in tissues of heart and brain. On the contrary, p38γ and p38δ show tissue-specific expression patterns: p38γ is highly expressed in skeletal muscle, whereas p38δ expression is concentrated in the kidneys, lungs, pancreas, testis, and small intestine [21]. In addition, p38γ expression can be induced during muscle differentiation. p38α and p38δ are abundantly expressed in macrophages, whereas p38β is undetectable. p38α and p38δ are also expressed in endothelial cells, neutrophils, and $CD4^+$ T cells, whereas p38β is abundant in endothelial cells. These findings indicate that, even though the four p38 family members share sequence homology, their expression is cell and tissue dependent, and their functions may therefore be different.

2.2 Mechanism of p38 response

p38 kinases are activated by environmental and cellular stresses including pathogens, heat shock, growth factors, osmotic shock, ultraviolet irradiation and cytokines. Moreover, various signaling events are able to stimulate p38 kinases, for example, insulin signaling. Interestingly, with respect to inflammatory responses, a number of studies have reported p38 regulation in macrophages treated with LPS, endothelial cells stimulated with TNF-α, U1monocytic cells treated with IL-18, and human neutrophils activated with phorbol 12-myristate 13-acetate (PMA), LPS,TNF-α, and fMLP [22, 23]. It should also be noted that p38 activation in different cell types is dependent on the type of stimulus. It has also been reported that distinct upstream kinases selectively activate p38 isoforms. p38 family kinases are all activated by MAP

kinase kinases(MKKs). MKK6 activates all four p38 isoforms, while MKK3 can activate p38α, β, and δ, but not p38γ [24], and MKK4 activates p38α and δ [25]. This indicates that p38 isoforms can be co-activated by the same upstream regulators and can be regulated specifically through different regulators. (Figure 1) [18]

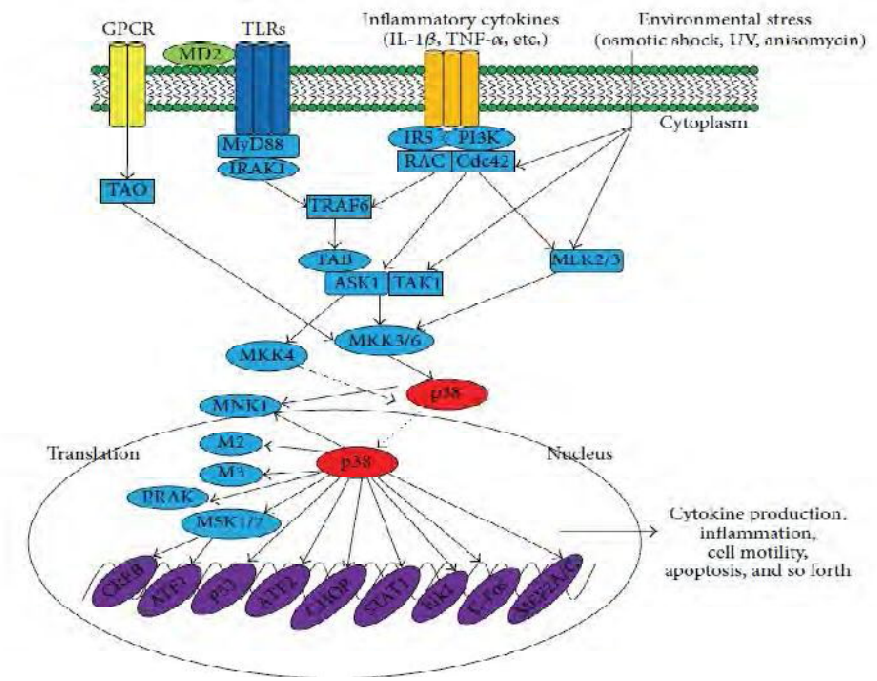

Figure 1 : p38-regulated signaling pathways in inflammatory responses. Inflammation-derived cytokines such as TNF-α and IL-1, TLR ligands such as LPS, poly(I:C), and peptidoglycan, as an environmental stresses, stimulate the phosphorylation of p38, leading to the activation of transcription factors such as AP-1 family. Subsequent expression of inflammatory genes by these transcription factors mediates various inflammatory responses including cytokine production, migration, and apoptosis of macrophages, monocytes, and neutrophils (18).

2.3 p38 inhibitors

Pyridinyl imidazole inhibitors contributed to the identification and characterization of the p38 pathway as a therapeutic target in inflammatory diseases [26]. Subsequently suitable modifications of the original structures yielded several pharmacological tools and early drug candidates such as

SB203580 [4-[5-(4-fluorophenyl)-2-(4-methylsulfinyl phenyl)-3H-imidazol-4-yl]pyridine] etc. These first-generation inhibitors were found, however, to be hepatotoxic and potential carcinogens owing to their potent induction of certain cytochrome P450 isoenzymes; thus, they have not been tried in the clinic [27].

There are >500 protein kinases in the human genome. Because of the high degree of structural similarity in the adenosine-binding pocket across the whole kinome, the design of specific kinase inhibitors targeted to the ATP site is a challenge in medicinal chemistry. It is presumed that exploitation of less-conserved surrounding areas, which are not used by ATP, can improve the selectivity. An example of success of this strategy is the drug Imatinib (STI571), which inhibits the tyrosine kinase BCR–ABL (breakpoint cluster region and Abelson murine leukemia viral oncogene homolog) – the causative agent in chronic myeloid leukemia [28]. By this extended strategy, pyridinyl imidazole inhibitors have been modified further, either by incorporating different substituents on the imidazole core or by replacing this core with different heterocycles. Structurally diverse new inhibitors have also been synthesized, including aryl amides and diaryl ureas, indolyl amides, 6,6-fused bicyclic core and related analogs, and ketone-derived inhibitors [29–33] (Figure 2).

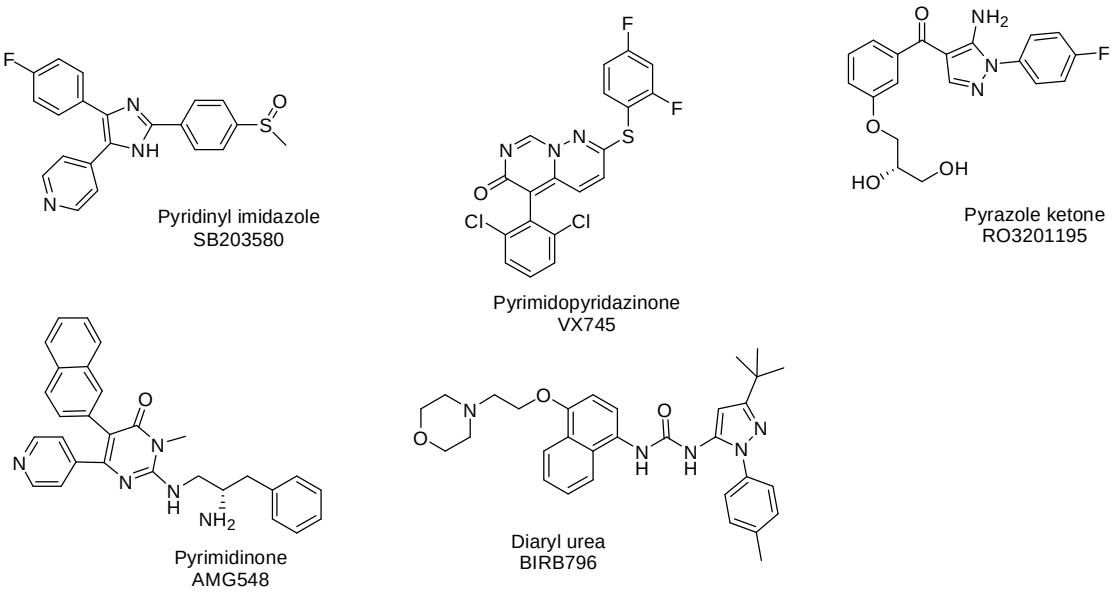

Figure 2: Structures of chemically different p38α inhibitors. Most of the currently available p38a inhibitors such as SB203580, RO3201195, VX745 and AMG548 bind competitively to the ATP site of the enzyme. Some (e.g. BIRB796) do not occupy more than a small corner of the adenosine pocket but their binding induces a conformational change that excludes ATP binding [33].

Several other compounds have been reported to be inhibitors of p38 MAP kinases but have failed to reach the market due to either lack of efficacy or toxicity issues [34-36].

Seiji Miwatashi [37] described the development of 4-phenyl-5-pyridyl-1,3-thiazoles as inhibitors of p38 MAP kinase with reduced side effects (reduced CYP3A4 activity). Among the various substituents studied, introduction of various phenyl amides along with small alkyl substituents on the pyridyl-thiazole core were found to have good cellular activity and pharmacokinetic profile. Among them, TAK-715 (Figure 3) was found to be a specific inhibitor of p38α MAP kinase with an IC_{50} value of 7.1 nM and exhibited inhibition of TNF-α production by 87.66% in mice with a 10 mg/kg single oral administration. It also showed a markedly reduced CYP inhibition and reasonable pharmacokinetics in both rats and mouse.

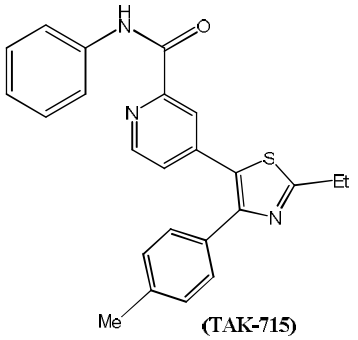

(TAK-715)

Figure 3

At our R & D Centre attempt was initiated to develop novel compounds as p38α MAP kinase inhibitors. It was decided to explore further the 4-phenyl-5-pyridyl-1,3-thiazole class of compounds by introducing a novel substituent on the C2 position of the pyridyl ring. Prior documents have indicated that the C2 substitution on the pyridyl ring is important for reducing CYP inhibitions while retaining the activity. The sulfoximine moiety (Figure 4) wherein, R_3 & R_4 independently represents alkyl, cycloalkyl or aryl groups which may be optionally substituted with halogen or alkyl groups was earlier explored as a substituent at our Centre for preparation of various anti-inflammatory compounds, one of which is presently in Phase II clinical trials as a dual COX/LOX inhibitor.

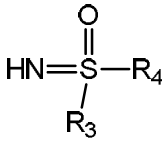

Figure 4

Therefore it was decided to incorporate the sulfoximine groups at the C2 position of the pyridyl ring.

Accordingly, a series of compounds were prepared with the following general structure (A, Figure 5) wherein R_1, R_3 & R_4 independently represents alkyl, cycloalkyl or aryl groups which may be optionally substituted with halogen or alkyl groups.

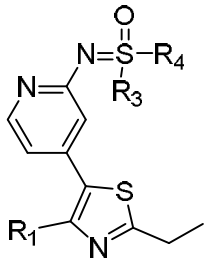

(A)

Figure 5

Initial docking studies with an alkyl group at R_3 & R_4 did not provide promising results. Interestingly, when a bulky phenyl group was attached as a substituent to the sulfoximine group on the C-2 position of the pyridyl ring, it adapted a different orientation compared to molecules mentioned in many of the earlier literature.

The compound **2**, wherein R_1 = Me, R_3 = Me, and R_4 is phenyl, (Figure 6)

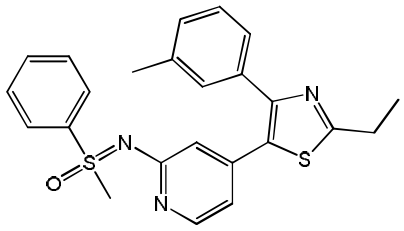

2

Figure 6

showed an IC_{50} of 1.1 μm in p-38 MAPK enzyme assay. Interestingly, the (S) isomer had an IC_{50} of 150 nm, while the (R) isomer was found to be less active. Several other compounds showed this trend leading to the understanding that the (S) conformation is therapeutically more preferred. Introduction of a bulky group at R_3 reduced activity. Thus, the compound **3**, where R_3 = cyclohexyl & compound **4** with R_3 = Ph (Figure 7) were found to be less active (IC_{50} = 12 μm

& 15 μm respectively)

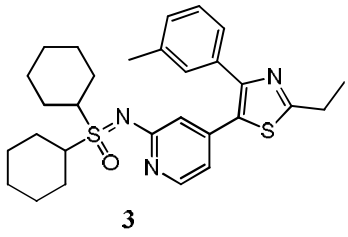

3

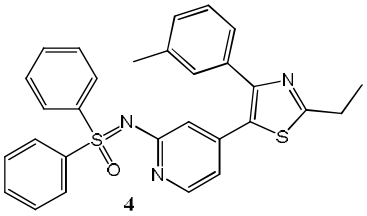

4

Figure 7

Replacement of R_3 with ethyl (**5**) and isopropyl (**6**) groups retained the efficacy while, the isobutyl group (**7**) (Figure 8), surprisingly, increased the IC_{50} value to 55 μm.

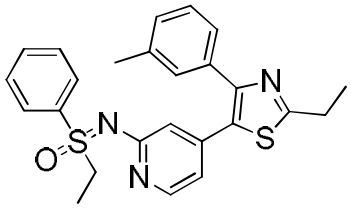

5

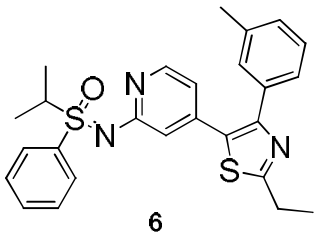

6

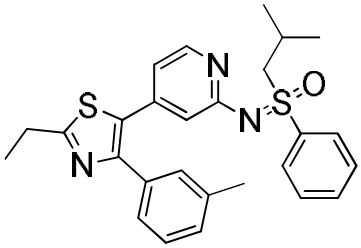

7

Figure 8

Further optimization of the SAR studies provided the following compound (**1**) as a specific inhibitor of p38α MAP kinase. Compound (**1,** Figure 9) was selected for further development.

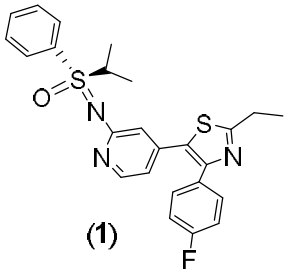

(1)

Figure 9

3 Studies on Compound (1) [R-(+)-S-(Isopropyl)-S-(phenyl)-N-[4-{2-ethyl-4-(4-fluorophenyl)-13,-thiazol-5-yl}-pyridin-2-yl]sulfoximine]

3.1 Chemistry and Rationale

The compound (**1**) exhibited an IC_{50} value of 7.1 nM and exhibited inhibition of TNF-α production by 43.3% in mice with a 10 mg/kg single oral administration in Balb/c mice.

The major challenges with further development of the compound **(1)** were:

- it is a thick viscous liquid, very unstable;
- upon storage even in air tight containers, it degraded and turned green;

Therefore, work was initiated to stabilize the base through either preparation of alternate polymorphic forms of the compound **(1)** or through salt formation

3.1.1 Molecular Modeling

In order to understand ligand binding mode and gain insight into the ligand-protein interactions docking studies were performed with compound (**1**) into the active site of P38-MAP kinase in complex with SB203580 ((pdb accession code 1A9U).

Top scoring pose of compound (**1**) adopts a conformation that allows it to form interactions with binding site residues i.e. Met109, Lys53. Thiazole N of ligand formed a hydrogen bond i.e. NH…O with side chain HN of Lys53. In addition to this, pyridine's 'N' formed a NH…N hydrogen bond with backbone NH of Met109. Upon superimposition, binding mode and H-bond interactions of compound (**1**) and bound ligand SB203580 as well as TAK 715 were found to be similar. (Figure 10)

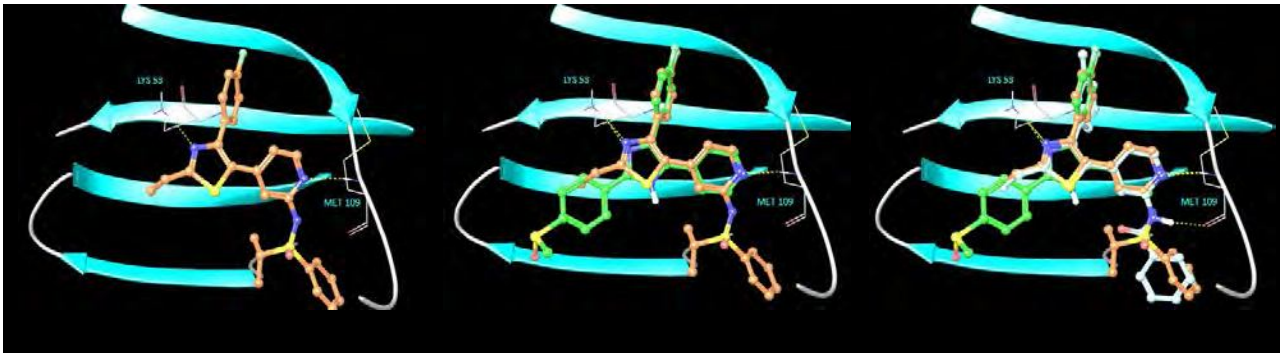

Comp. 1 | Comp. 1 with SB203580 | Comp. 1 with SB203580 and TAK715

Figure 10: binding mode and H-bond interactions of compound (1) and bound ligand SB203580 as well as TAK 715

3.1.2 Synthetic process

The initial synthesis of compound **(1)** was done according to the Scheme-1. The final product was obtained by chiral separation of the racemate using chiral column chromatography.

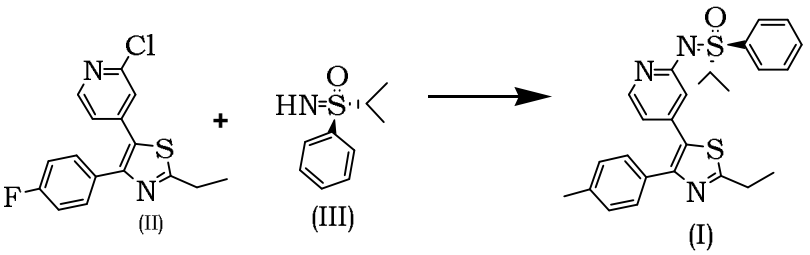

Preparation of Intermediate (III):

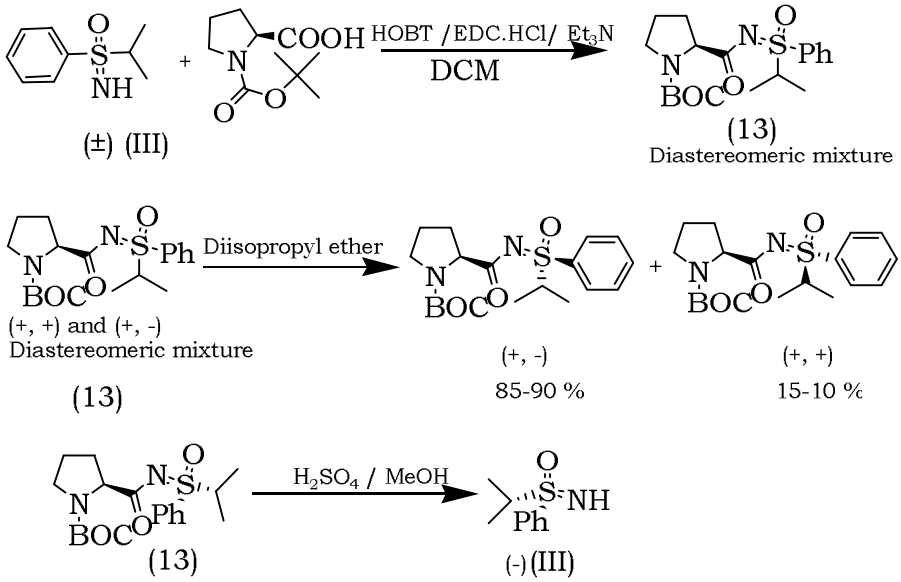

Scheme 1 : Preparation of compound of formula (I)

The chloro intermediate (II) was sourced commercially and was reacted with the chiral sulfoximine of formula (III) to obtain the final compound (I). However, the yields were low (~15-18%).The racemic sulfoximine (III, **9**) was prepared using standard technique for preparation of sulfoximines as shown in Scheme-3.The resolution of racemic (III) was initially carried out using L-Boc proline by peptide coupling method using EDC/HOBT to form the amide (**13**) as a mixture of diastereoisomers. The diastereoisomers were separated using diisopropyl ether. The major diastereoisomer is hydrolysed to get the (-) isomer of (III).

The process suffered from the following disadvantages:

- The yield using the chloro intermediate (II) was low;

- Required column chromatography for purification which is difficult to use in plant scale;
- The process of resolution of (III) using N-boc-L proline is difficult in industrial scale.

Therefore, an alternate synthetic route was designed as follows (Scheme 2):

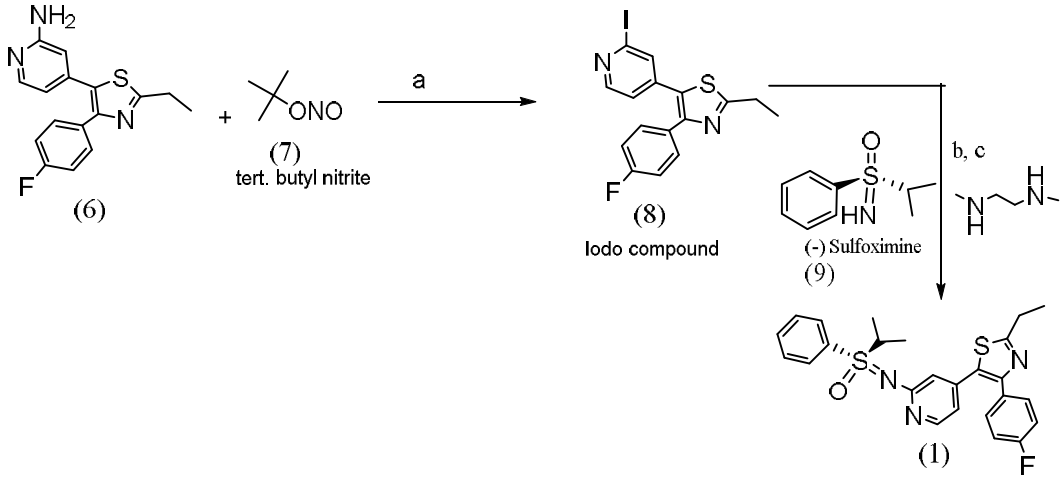

Reagents & conditions: a. I_2, CH_2I_2; b. CuI, Cs_2CO_3; c. toluene, 100-110℃

Scheme 2: Synthesis of compound (1)

The compound **(6)** was obtained from commercial sources. It has been reported that while carrying out a variation of Buchwald-Hartwig coupling as used in Scheme 1 above for cross coupling of the imine (III) with (II), the iodo intermediates are preferred over the chloro intermediate (38).Accordingly, the synthesis of the iodo intermediate instead of the chloro intermediate (III) of scheme 1 was carried out by standard diazotization reaction by reacting **(6)** with tertiary butyl nitrile **(7)** as described in Scheme 2. The obtained product, compound of formula **(8)** is new. The use of tert-butyl nitrile and iodine for iodination of a secondary amine is well reported. During optimization of reaction conditions for the synthesis of **(8)**, several solvent systems and range of reaction temperature were tried. Use of diiodomethane at 75 ℃ was found to be optimum which gave 40 % yield.

The (-) sulfoximine **(9)** was prepared as per the following Scheme 3:

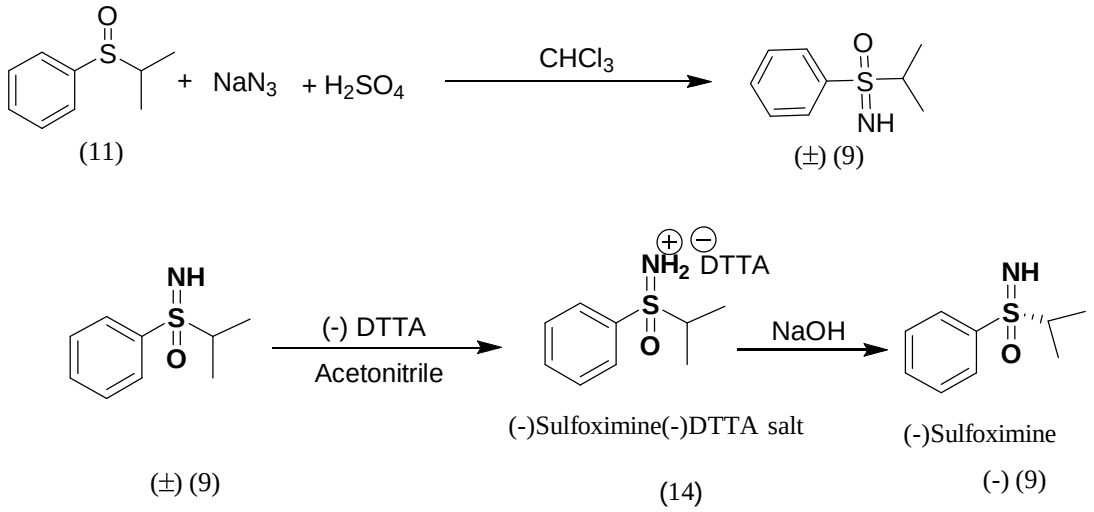

Scheme 3: Preparation of (-) 9

The racemate of the sulfoximine compound **(9)** was prepared by known processes. However, resolution of the racemate sulfoximine posed another challenge. Several resolving agents & reaction conditions were tried before it was possible to obtain the (-) isomer in good yield with high chiral purity by using the ditolyl tartaric acid (DTTA) in acetonitrile. The DTTA salt of (-) **(9)** precipitated out which was filtered and hydrolysed with NaOH to obtain the (-) **(9)**. Subsequent reaction of the (-) sulfoximine **(9)** with compound of formula **(8)** was done as per general process described by Jörg Sedelmeier and Carsten Bolm [39], to provide the compound of formula **(1)** as oil. The compound **(1)** was difficult to purify. It turned green on storage and degraded quickly. Initial attempts to obtain it in a solid form were not successful. Several solvents were tried. Crystallization was also attempted at various temperatures but was unsuccessful. Some of the solvents which were attempted are diisopropyl ether, lower alcohols, THF, MTBE etc. Finally, the base could be crystallized from n-heptane by keeping the solution undisturbed for more than fifteen days. However, it was hygroscopic upon storage.

Therefore, attempts were made to convert the compound **(1)** into its pharmaceutically acceptable salts. Over twenty different salts were tried but

due to the inherent instability of the compound **(1)**, only a few salts could be isolated. The salts were prepared by reacting with corresponding acids in suitable solvents and stirring at 5-10 ℃ to room temperature and then separating the salt formed.

4 Results and discussion

The process of Scheme-2 gave the final compound (**1**) in good yield (~70%). The compound was obtained in good chemical and chiral purity. The process did not require column chromatography. The resolution of **(9)** using (-)DTTA salt in acetonitrile gave the (-) **(9)** sulfoximine in good yield (64%) and chiral purity (71%). The chirality of the crystalline base was confirmed through single crystal structure elucidation (figure 11) which confirmed the (S) configuration.

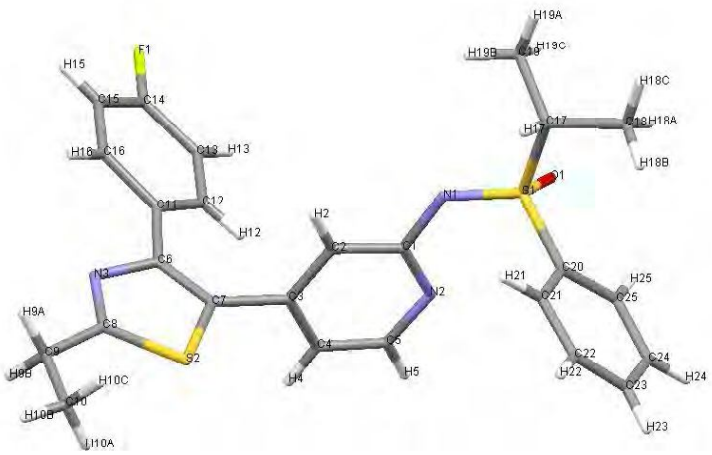

Figure 11: Single crystal structure of compound (1)

Of the various salts attempted, only the following salts (Table 2) could be isolated in solid form:

Table 2: Salts of compound (1):

Sl. No.	Salt prepared	Melting point °C	Nature
1.	Hydrochloride (1a)	Onset = 109.4 °C Peak = 111.0 °C	Amorphous
2.	Para-toluene sulfonic acid (PTSA) (1b)	120 °C (diffuse)	Amorphous
3.	Bisulfate (1c)	Onset = 182.9 °C Peak = 187.0 °C	Crystalline
4.	Phosphate (1d)	Onset = 114.2 °C Peak = 126.7 °C	Amorphous
5.	Citrate (1e)	60-66 °C (by apparatus)	Amorphous

Of these, the citrate salt was hygroscopic, the phosphate and PTSA salts became sticky when exposed to atmosphere. The bisulfate salt **(1c)** was found to be the most stable and obtained in a crystalline form. The HCl salt was amorphous in nature.

a) Efficacy studies:

The efficacy of the compound (1) and various salts were studied as follows:

In the first experiment, the salts and the base were tested for their ability to inhibit LPS induced TNF-alfa activity in human whole blood assay ex-vivo. The results are provided in Table 3:

Table 3: Evaluation of LPS induced TNF-alpha inhibitory activity of compounds in human whole blood assay

Sl. No.	Sample	Conc. (µM)	% inhibition	
			Mean	S.E.M.
1.	Prednisolone	0.3	74.4	1.3
		3	91.9	0.8
2.	Compound (1)(base)	3	62.4	17.8
		30	93.5	3.7
3.	HCl salt (1a)	3	47.0	0.4
		30	96.4	0.1
4.	PTSA salt (1b)	3	47.2	16.6
		30	95.5	1.8
5.	Bisulfate salt (1c)	3	53.1	14.8
		30	93.4	0.5
6.	Phosphate salt (1d)	3	64.5	14.6
		30	94.6	3.4
7.	Citrate salt (1e)	3	45.4	8.42
		30	96.0	0.32

*SEM: standard error of the mean

The bisulfate salt **(1c)** of the compound **(1)** was stable, obtained in crystalline form and was found to be a potent inhibitor of p38 MAP kinase.

The compound **(1c)** was next tested *in vivo* in suitable animal models. The compound showed good inhibition in rat paw edema (RPE) model when tested in Female Wistar rats (Table 4) and Figure 12.

Table 4: Rat paw edema studies in female Wistar rats

Treatment group	% inhibition of paw edema		
	1 hr.	3 hr	5 hr
Compound 1(c) (3 mg/kg p.o.)	-12.11±3.95	-0.05±4.65	-5.98±3.61
Compound 1(c) (10 mg/kg p.o.)	21.33±6.89	12.19±3.17	1.54±5.16
Compound 1(c) (30 mg/kg p.o.)	50.00±4.50	21.92±3.38	17.00±3.84
Compound 1(c) (100 mg/kg p.o.)	55.53±3.78	34.77±2.17	21.08±3.14

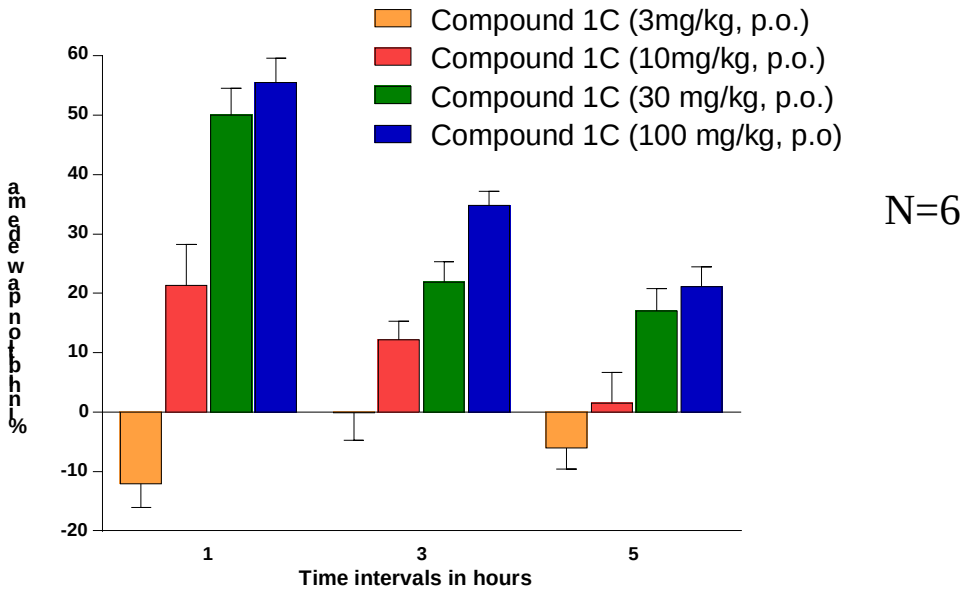

Figure 12: RPE profiling in Female Wistar Rats at different time points

When compared to TAK-715, compound (**1c**) showed superior efficacy in RPE model at different time points as shown in Table 5 and Figure 13.

Table 5: Comparison of Compound (1c) with TAK-715 in RPE model inFemale Wistar Rats

Sl. No	Treatment group (mg/kg, p.o.)	% inhibition paw edema								
		1hr			3hr			5hr		
1	TAK-715 (30)	38.87	±	9.29	17.17	±	3.27	10.21	±	2.15
2	Compound 1(C) (30)	53.11	±	6.58	25.97	±	1.54	12.75	±	2.46

N=6

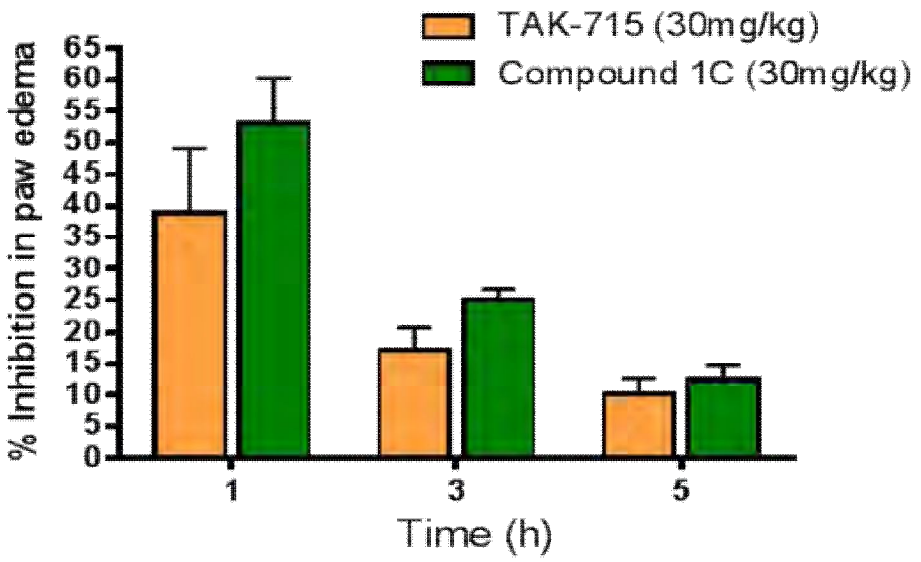

Figure 13: Comparison of Compound (1c) with TAK-715 in RPE model inFemaleWistar Rats

The efficacy of the compound **(1c)** in terms of its *in vivo* anti-inflammatory activity was further tested in *Streptococcus pyrogenes* induced arthritis model

in streptococcal cell wall (SCW)-primed SD (Sprague-Dawley) rats. Tak-715 was used as a comparator. The results are provided in Figure14.

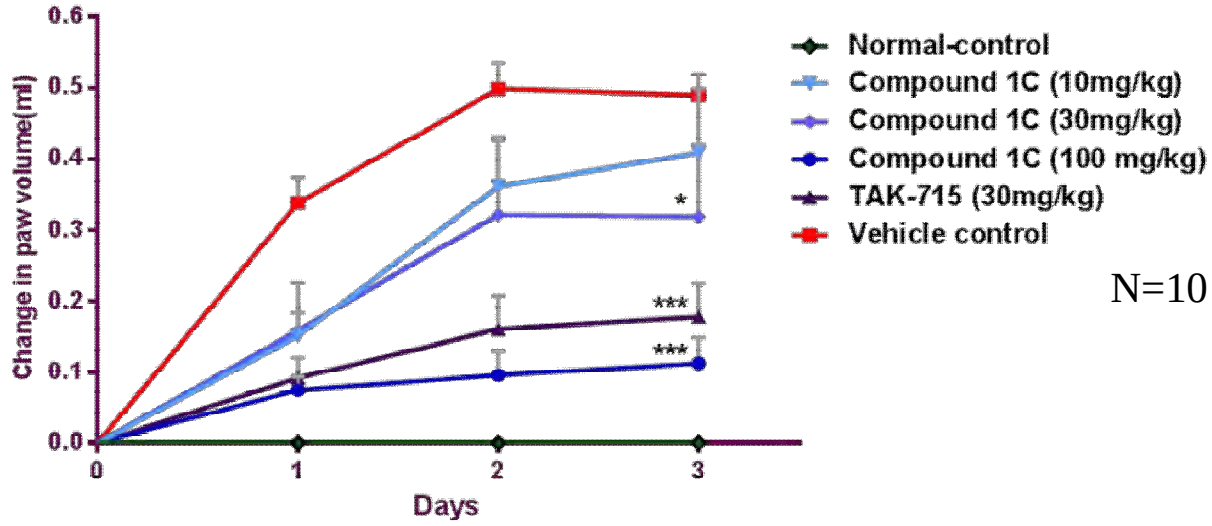

Figure 14: Comparison of compound (1C) with TAK-715 in SCW model

The compound **(1c)** showed good reduction in paw volume when compared to TAK-715.

b) Pharmacokinetic studies:

The compound **1(c)** also showed good pharmacokinetic profile both in various species as seen in Table 6below:

Table 6: Pharmacokinetic of Compound 1(c) in different animal species

Compound	Animal No.	Dose (mg/ Kg)	Tmax (hr)±SD	Cmax (µg/ml)±SD	T1/2 (hr)±SD	AUC (0-t) (hr.µg/ml)± SD	AUC (0-∞) (hr.µg/ml)± SD
1(c)	W.rat (N=4)	30	2.00 ± 1.41	0.27± 0.13	3.19 ± 0.49	1.17 ± 0.25	1.44 ± 0.41
1(c)	W.rat (N=6)	30	4.00 ± 0.0	0.35 ± 0.06	7.15 ± 1.14	2.14 ± 0.31	2.45 ± 0.31
1(c)	Balb/c mice	30	0.25 ± 0.09	0.62 ± 0.15	0.86 ± 0.07	0.68 ± 0.06	0.71 ± 0.07

	(N=24)						
1(c)	Beagle Dog (N=2)	10	0.33 ± 0.0	0.24 ± 0.01	2.37 ± 0.35	0.56 ± 0.06	0.65 ± 0.11

5 Conclusion:

The compound of formula (**1**) was difficult to obtain in solid form. The crystalline form was unstable and difficult to store. Attempts to obtain alternate crystalline forms were therefore not attempted. The compound (**1**) was stabilized through salt formation. The bisulfate salt (**1c**) was obtained in crystalline form and was found to be stable. It showed good anti-inflammatory properties both *in vitro* and *in vivo*. Further, it showed good pharmacokinetics profile across species. Based on all of these the bisulfate salt (**1c**) of compound **1** has been selected for further development.

6 Experimental Section:

6.1 Synthesis

6.1.1 Synthetic Materials and Methods

Reagents and solvents were obtained from commercial suppliers and used without further purification. Flash chromatography was performed using commercial silica gel (230-400 mesh). Melting points were determined on a capillary melting point apparatus and are uncorrected. IR spectra were recorded on a Shimadzu FT IR 8300 spectrophotometer (Vmax in cm^{-1}, using KBr pellets or Nujol). The ^{1}H NMR spectra were recorded on a Brucker Avance-300 spectrometer (300 MHz). The chemical shifts (δ) are reported in parts per million (ppm) relative to TMS, either in $CDCl_3$ or DMSO-d_6 solution. Signal multiplicities are represented by s (singlet), d (doublet), dd (doublet of doublet), t (triplet), q (quartet), bs (broad singlet), and m (multiplet). $^{13}CNMR$ spectra

were recorded on Brucker Avance-400 at 100 MHz either in $CDCl_3$ or DMSO-d_6 solution. Mass spectra (ESI-MS) were obtained on Shimadzu LC-MS 2010-A spectrometer. HPLC analysis were carried out at λ_{max} 220 nm using column ODS C-18, 150nm * 4.6 nm * 4 μ on AGILENT 1100 series.

6.1.2 Preparation of compound of formula (8)

Step 1

Preparation of Tert. butyl nitrite (7)

Placed sodium nitrite (5.135 Kg) in water (2.027 L) and contents were cooled at –5 to 0 °C. To the solution was added dropwise a cooled (0 °C) mixture of t-BuOH (5 Kg) and aq. H_2SO_4 (3.378 Kg) at –5 °C for over 2 hrs. After completion of addition the two phase solution was stirred at 0 °C for another 1 hour. The two phases were separated. The yellow organic phase was washed with mixture of aq. $NaHCO_3$ and NaCl solution (1L), dried over sodium sulphate and stored at –10 to 0 °C (4.25 Kg).

Step 2

Preparation of 4-[2-ethyl-4-(4-fluoro-phenyl)-thiazol-5-yl]-2-iodo- pyridine (8)

The iodo compound **8** was prepared by reacting the amine intermediate of formula **6** with the tert butyl nitrile **7** and iodine in the presence of suitable solvent. Initial reactions using methylene chloride were not successful and provided product with low yields. The reaction is exothermic and it was difficult to control. Also, the reaction required very high mole excess of t-butyl nitrite (8 Meq) and the reaction time was quite high (16 hours at RT). The product was purified by column chromatography but still was reddish in colour. To overcome these problems several modifications of the reaction conditions were tried. Initially, the reaction was carried out in different solvents and also the reaction temperature was altered as provided in Table 7 below. It was found that higher temperature was more suitable.

Table 7: Screening of solvents for preparation of compound (8):

Solvent	Temperature (°C)	Yield
Methylene Chloride	25	10%
Chloroform	25	<10%
Methylene Chloride	70	25%
Acetonitrile	27	15%
Ethylene glycol	65	32 %
Toluene	70	30%
Benzene	70	27%
Methyl iodide	70	36%
Diiodomethane	75	40%

Increasing the reaction temperature to 70-75 °C also reduced the reaction time to about 2-3 hours. In a second effort at optimization, the mole proportion of the amine **6**, t-butyl nitrite **7** and iodine were varied. Several alternatives were tested by varying the mole proportion of the nitrile and iodine. A mole ratio of 1:2:1 was found to be optimum. The purification process was optimized performing column chromatography using SS316 Naustch filter and vacuum instead of glass column and air pressure. Various solvents were attempted for eluting the product as provided in Table 8:

Table 8: Screening of solvent(s) for elution of compound (8):

Sl. No.	Solvent/solvent mixture	Elute
1.	Hexane	Diiodomethane
2.	4 % EtOAc	Mixture of impurities
3.	4% EtOAc in Hexane	Non-polar impurities
4.	6% EtOAc in Hexane	Product (IIA) with non-polar impurities
5.	10-20% EtOAc in Hexane	Iodo product (IIA)

In an interesting observation it was found that the mode of addition of the reagents also played a crucial role in helping control exothermicity. Thus, when the amine **6** was added to a mixture of t-butyl nitrite, iodine and diiodomethane, the exothermic reaction could be controlled. The reddish colour was removed by washing with suitable weak base, preferably by washing with sodium bisulfite solution.

Process:

To a mixture of diiodomethane (12.5 Kg) and iodine (0.850 Kg), was added dropwise tert-butyl nitrite (0.750L) over a period of 1 h at 25 – 30 °C (exothermic). To the reaction mixture was added 4-[2-ethyl-4-(4-fluorophenyl)-1,3-thiazol-5-yl]pyridin-2-ylamine (1 Kg) at room temperature (28 °C) in one lot. The mixture was heated to 70 - 75 °C for 1 h.

Mobile phase (for TLC): Ethyl acetate: hexane (1:1)

After completion, the reaction mixture was dumped into saturated sodium bicarbonate solution (20 L). To the solution was added dropwise saturated solution of sodium thiosulphate (5 L) at RT. The mixture was stirred for 1h to remove colour of iodine. The suspension was filtered on hyflo powder. Subsequently it was washed with ethyl acetate (1.25 L). The solvents were evaporated under reduced pressure. After complete removal of diiodomethane, the contents were extracted with ethyl acetate (15 L) and chloroform (2 x 5 L). The combined organic layer was washed with saturated aq. $NaHSO_3$ (5 L), water (5 L) and 5% brine solution (10 L), dried over anhydrous sodium sulphate, filtered through hyflow and solvents were evaporated under reduced pressure to yield dark brown semi solid.

Purification:

The crude product was adsorbed over silica-gel (220-400) (2 Kg). It was filtered over Naustch filter using vacuum. Elution with 5-20 % EtOAc in hexane yielded desired iodo compound. Wt. pure product: 0.645 Kg (42 %).

^{1}H NMR ($CDCl_3$, 300MHz): δ1.44 (t, 3H), 3.07 (q, 2H), 7.02-7.07 (m, 2H), 7.10-7.11 (m, 1H), 7.43-7.49 (m, 2H), 7.65-7.66 (m, 1H), 8.22-8.24 (m, 1H).

^{13}C NMR ($CDCl_3$): 14.09, 27.13, 115.63, 115.84, 118.46, 122.75, 126.75, 130.05, 130.95, 134.15, 141.97, 150.65, 151.14, 161.63, 164.10, 173.079.

6.1.3 Preparation of R- (-)-S-Isopropyl-S-phenyl sulfoximine (9)

Step 1:

Preparation of racemate of the sulfoximine compound of formula (9)

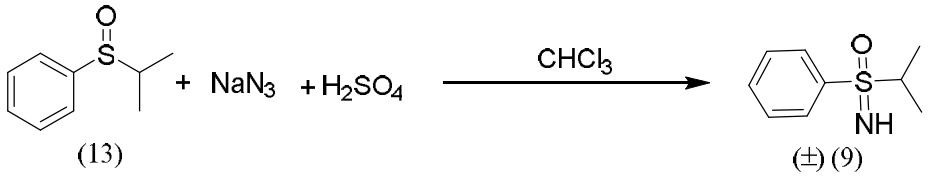

(13) (±) (9)

The compound of formula (±) **9** was prepared by known processes [40, 41]. The process comprises slow addition of sulfuric acid to the Isopropyl-sulfinyl-benzene**13** in chloroform. It was observed that if conc. H_2SO_4 is added rapidly, the suspension (reaction mixture) turns pale brown to dark brown when brought at room temperature, and non-polar impurities are generated whereby the reaction has to be discarded. Subsequently sodium azide is added to the reaction mixture to obtain the racemic sulfoximine of formula **9**. The crude sulfoximine was purified by dissolving in methanol and isolated as the hydrochloride salt which was subsequently basified to obtain pure racemate of **9**.

6.1.4 Preparation of (-) sulfoximine of formula (9)

Various resolving agents for resolution of (**9**) were tried e.g. tartaric acid, Camphor sulfonic acid, mandelic acid etc. (-) di-p-tolyl tartaric acid (DTTA) in suitable solvents was found to be useful. The various solvents tried are listed in Table 9.

Table 9: Solvent screening for preparation of R-(-)-S-(Isopropyl)-S-(phenyl)-sulfoximine (12) through formation of the DTTA salt

Sl. No.	Racemic Sulfoximine	(-) DTTA acid	Solvent	Diasteriomeric salt	Yield (%)	Chiral purity (ee)
1.	600 mg	1.393 g (1.1 eq.)	Acetone/DIPE	800 mg	43	37.72 %
2.	800 mg	1.69 g (1.0 eq.)	Acetone/EA	270 mg	11	51.68 %
3.	115 mg	121 mg (0.5 eq.) +17 mg Formic acid (0.5 eq)	Methanol/ DIPE	110 mg	31	32.7 %
4.	910 mg	2.11 g (1.1 eq.)	Acetone/CAN	940 mg	33	46.12 %
5.	347.7mg	806.7mg(1.1)	Isopropyl Acetate/DIPE	705mg	37	58.48%
6.	1.07g	2.479gm	Acetonitrile/DIPE	2.312	70	55.14
7.	2.1gm	3.32gm (0.75eq)	Acetonitrile	1.3gm	20.0 %	71.68
8.	5.2 g	5.54 g (0.5 eq.)	Acetonitrile	5.2 g	64.4 %	71.2

Thus, acetonitrile was selected as the optimal solvent. A mixture of acetone and isopropyl ether (IPE) improved the yield significantly but the chiral purity was compromised. It was also found that use of 0.5 mole equivalent of the (-) DTTA increased the yield significantly while retaining the chiral purity. Accordingly,

the resolution was carried out using 0.5 mole equivalents of (-)-DTTA in acetonitrile. The DTTA salt was subsequently treated with aqueous NaOH to obtain the chiral sulfoximine of formula (**9**) having chiral purity of 93.57 % and HPLC purity of 99.7 %.

Process:

Take 835 mg racemic sulfoximine of formula (**9**) (4.557 mmoles) and dissolve it in 5 ml. acetone. Stir the reaction mass at 45-50 °C and add to it 1.758 gm (4.551 mmoles) of (-) Di-p- tolyl-L-tartaric acid in a single lot. First clear solution was formed. After 20 minutes a white precipitate was observed. The mixture was cooled at 25-30 °C and filtered. The solid mass was washed with 10 ml acetone. The crude DTTA salt obtained was purified by recrystallization in acetone to increase the chiral purity.

Weight of the diastereomeric salt: 1.780 gm;

Chiral purity: e.e.> 97%.

Neutralization of the above diastereomeric salt by adding 10 % NaOH solution till pH becomes basic in DCM & water system provides the free chiral sulfoximine.

Weight of (-) sulfoximine: 350 mg;

Chiral purity: e.e.> 97%.

6.1.5 Preparation of R-(+)-S-(Isopropyl)-S-(phenyl)-N-[4-{2-ethyl-4-(4-fluorophenyl)-13,-thiazol-5-yl}-pyridin-2-yl]sulfoximine (1)

The compound **1** was prepared by following the general process described by Jörg Sedelmeier and Carsten Bolm [39]. 4-[2-ethyl-4-(4-fluoro-phenyl)-thiazol-5-yl]-2-iodo- pyridine **8** was treated with R-(-)-S-(Isopropyl)-S-(phenyl)-sulfoximine **9**, copper (I) iodide, cesium carbonate and *N, N'*-Dimethyl ethylene diamine in suitable solvent and the mixture was heated for extended period to

obtain the compound **1** as an oil. The reaction was also dependent on the solvent being used and various solvents were tried as provided in the Table 10 below.

Table 10: Solvent screening for preparation of compound of formula (1)

Sl. No.	Iodo compound (9)	Sulfoximine (12)	Solvents	Yield	% purity
1.	959 mg (HPLC= 88.0 %)	377 mg	Toluene	1.05 g	HPLC = 86.31%
2.	55.9 mg	25 mg	DMF	No reaction	---
3.	959 mg	377 mg	Toluene	925 mg (Crude) 350 mg (Pure)	HPLC = 91.44%
4.	500 mg	233 mg	Toluene	417 mg	HPLC = 97.37% Chiral= 87.16 %
5.	500 mg	223.3 mg	Benzene	350 mg	HPLC=99.1 % Chiral=70%
6.	20.82 g	9.3 g	Cyclohexane	19.0 g	HPLC = 98.99 % Chiral = 85 %

Based on the above, cyclohexane was used as the solvent and when the mixture was heated at 80 °C, the reaction time was reduced to 8-10 hours.

Process:

Placed 4-[2-ethyl-4-(4-fluoro-phenyl)-thiazol-5-yl]-2-iodo- pyridine (9, 34.5 g), R-(-)-S-(Isopropyl)-S-(phenyl)-sulfoximine (12, 13.9 g), copper (I) iodide (cuprous iodide, 4.8 g), cesium carbonate (69 g) and *N, N'*-dimethyl ethylene diamine (4.8 mL) in toluene (200 mL) and reaction mixture was heated at 100-110°C with stirring overnight.

After completion, the content were poured over water and filtered over hyflo, aq. layer extracted with ethyl acetate. The combined organic extract was washed with water, brine, dried over sodium sulphate and solvents were evaporated under reduced pressure to yield brown oil (48 g)

Purification

The crude product was adsorbed over silica-gel (230-400). Elution with 20 % ethyl acetate: hexane yielded desired product. The pale-yellow oil was stirred in hexane: di-isopropyl ether (50 mL, 100:5) overnight. The white-off-white solid was filtered, washed and dried under reduced pressure. This solid compound was found to be unstable and readily decomposed on exposure to air.

Wt. of product: 22.5 g

6.1.6 Preparation of crystalline compound (1)

Procedure:

200 mg of the chirally impure compound of formula **1** obtained above (chiral purity 85:15) was dissolved in n-heptane (25 ml) & stirred till a clear solution was formed. The clear solution was kept at room temperature (25-30 °C) for 10-15 days, when a white needle shaped crystalline solid mass appeared. On the wall of the conical flask a spherical shape solid mass was deposited, and at the centre of the flask needle shaped crystals were formed. The two crystalline masses were analyzed separately.

Analysis showed that the needle shape crystals are 100 % chirally pure (chiral HPLC = 100 %; chemical HPLC = 99.61 %) while the spherical shaped solid crystals were the racemic compound (chiral HPLC = 53:47).

i) M.P = 108-110 °C

ii) ESI-MS = 465.9 $(M+H)^+$

iii) MF: $C_{25}H_{24}FN_3OS_2$; MW: 465.11

iv) NMR :400 MHz (δ in $CDCl_3$)

1.28-1.26 (d , *J* = 6.8 Hz, 3H), 1.44 -1.41 (dd , *J* = 7.6, 6.8 Hz, 6H),7.88-7.86 (d , *J* = 7.6 Hz, 2H),3.08- 3.02 (q , *J* = 7.6, 7.6 Hz, 2H), 3.62- 3.59 (t , *J*= 6.8, 6.8 Hz, 1H), 6.56- 6.55 (d , *J*= 4.4 Hz, 1H), 6.85 (s, 1H), 6.99-6.92 (t, *J*= 8.7 Hz & 8.8 Hz, 2H), 7.46 -7.42 (dd , *J*= 5.6, 3.2 Hz, 2H),7.54 -7.51 (dd , *J* = 8, 3.2 Hz, 2H),7.61-7.59 (d, *J* = 7.2 Hz, 1H), 7.88-7.86 (d , *J* = 7.6 Hz, 2H), 7.96-7.94 (d, *J* = 5.2 Hz, 1H).

6.1.7 Preparation of HCl salt (1a):

0.5 gm of compound **1** prepared above was dissolved in methanol (10 ml). It was stirred at 5-10 ^{0}C using a magnetic stirrer for 10 minutes and to it was added methanolic HCl at 5-10 ^{0}C with stirring till the pH became acidic. The solution was stirred for 20 minutes at 5-10 ^{0}C. Subsequently, the solution was evaporated on a rotavapour and the solid was isolated.

Yield: 2.0 g

Table 11: Preparation of HCl salt of compound 1

Batch No.	Quantity	M.P.	% Chloride by IC	% water by KF
1	2.172 g	78-80 °C	9.49%	-
2	1.2 g	78-85 °C	10.61%	-
3	1.0 g	78-85 °C	9.60%	-
4	2.5 g	80-85 °C	10.62%	1.04%
5	3.0 g	80-84 °C	8.15%	-

6	6.7 g	80-84 °C	10.2%	-

The HPLC purity was found to be more than 98% for all the batches.

6.1.8 Preparation of para-toluenesulfonate salt (1b):

0.5 gm of compound **1** prepared above was dissolved in 10 ml of acetone. It was stirred at 5-10 ^{0}C using a magnetic stirrer for 10 minutes. To it was added 204 mg of para-toluene sulfonic acid (PTSA) dissolved in 2 ml of acetone. The solution was stirred for 30 minutes at 5-10 ^{0}C. Subsequently, the solution was evaporated on a rotavapour and the solid was isolated.

Yield: 1.4 g

6.1.9 Preparation of the bisulfate salt (1c):

0.5 gm of the free base **1** was taken in methanol. To it was added methanolic H_2SO_4 at 5 – 10 ^{0}C till the solution turned acidic. The solution was stirred for 30 minutes using a magnetic stirrer. Subsequently, the solution was evaporated on a rotavapour to obtain the bisulfate salt.

Table 12: Preparation of bisulfate salt of compound 1:

Batch No.	Quantity	M.P.	% sulfate by IC	% HPLC
1	1.170 g	175-177 °C	32.33 %	99.18%
2	14 g	173-175 °C	28.41%	99.23%
3	104 g	173-175 °C	27.88%	98.61%
4	8 g	173-175 °C	-	-
5	275 g	173-175 °C	30.98%	99.06

6.1.10 Preparation of phosphate salt (1d):

0.5 gm of compound **1** prepared above was dissolved in 10 ml of ethanol. It was stirred at 5-10 ^{0}C using a magnetic stirrer for 10 minutes. To it was added phosphoric acid (H_3PO_4) dropwise till acidic. The solution was stirred for 30

minutes at 5-10 ^{0}C. Subsequently, the solution was evaporated on a rotavapour and the solid was isolated.

Yield: 0.6 g (Mo. Wt. 560.6)

6.1.11 Preparation of the citrate salt (1e):

0.5 gm of the free base **1** was taken in toluene. To it was added citric acid dissolved in toluene at room temperature till the solution turned acidic. The solution was stirred for 60 minutes using a magnetic stirrer. Subsequently, the solution was evaporated on a rotavapour to obtain the citrate salt.

Table 13: Preparation of citrate salt of compound 1:

Batch No.	Quantity	M.P.	% HPLC
1	175 mg	60-66 °C	98.30%
2	130 mg	60-66 °C	98.85%

6.2 Biological studies on compound of formula (1) and its various salts.

6.2.1 Evaluation of LPS induced TNF-alpha inhibitory activity of compounds in human whole blood assay

Two microliters of the vehicle /NCEs/prednisolone was incubated in duplicate with the human whole blood at 37 °C for 1hr. After incubation, LPS (1ng/ml, final concentration) was added in the blood sample. It was further incubate for 5 hr at 37 °C. After completion of 5h, blood samples were transferred into ice bath to stop the release of TNF-α. Samples were then centrifuged at 3500 rpm for 10 minute at 4 °C. Plasma was separated & stored in deep freeze till the estimation of TNF-α by using commercially available TNF-α kits (BD Biosciences).

The plasma was diluted 25 times with assay diluent for estimation of TNF-α. The reagent preparation and assay procedure was performed as per manufacturer's (BD Biosciences) instructions.

6.2.2 Paw Edema study:

Male wistar rats were weighed on the day of experiment and based on which the volume of formulation was calculated so as to administer a single dose of the specified mg/kg of body wt. The animals were dosed in the morning one-hour before to carrageenan injection (1% w/v, 0.1ml/rat sub-planterly). The Paw volume was measured one hour before and at 0, 1, 3 & 5 hour after Carragenan injection using Ugobasile Plethysmometer

6.2.3 SCW induced arthritis in SD rats study:

Female Sprague dawley rats were primed with an intra-articular injection of 20µl of PGPS (peptide glycan polysaccharide) at 0.5 mg/ml of rhamnose solution in the right ankle. At 2 weeks the paw swelling were measured with plethysmometer and rats assigned to groups of similar distribution of initial paw swelling. Rats then received their first dose of compound followed 1 h later by an i.v. injection of 0.5 ml of PGPS (0.5 mg/ml of rhamnose solution) in the tail vein. Compounds were dosed and paw volume measured for 3 days.

6.2.4 Pharmacokinetic studies:

Pharmacokinetics of the test compound was studied via per-oral route of administration in appropriate species (wistar rats of 8 to 10 weeks of age or beagle dogs). Animals were fasted for 18 hours and food was supplied after 4 hours of administration of the test compound. There was free access to water throughout the study. A homogenous suspension of the test substance was prepared in 0.5 % w/v CMC in normal saline and a per-oral dose of 30 mg/kg was administered. After the administration of the test compounds, blood samples were withdrawn at various time intervals through retro-orbital plexus

and collected into heparinized micro centrifuge tubes. Plasma was separated by centrifugation at 4000 rpm for 5 min at ambient temperature and analyzed immediately. Remaining samples were stored at -20 °C until analyzed.

Analysis was carried out by taking an aliquots of 180 µL plasma and 20 µL of internal standard (Atorvastatin) and was extracted with 2.5 mL of extracting solvent (ethyl acetate: acetonitrile 80:20, v/v) in glass test-tube by vortexing with spinix vortex mixture for a minute. This was then centrifuged at 2000 rpm for 2.0 min. The supernatant was transferred to another glass test-tube and the solvent was evaporated under nitrogen using Zymark evaporator at 40 °C. Finally, the tubes were reconstituted with 0.1 mL diluent (acetonitrile: methanol: water 40:40:20, v/v/v). The reconstituted samples were analyzed on Agilent 1100 Series HPLC system with a mobile phase of 0.05 % v/v trifluoroacetic acid in water: acetonitrile (32:68, v/v); flowing at a flow rate of 1.0 mL/min through a Kromasil 250 mm x 4.6 mm x 5 µ column maintained at 30 °C. Chromatographic separation was achieved within 15 min. Agilent software version Chemstation Rev.A.09.01. (1206) was used to acquire and process all chromatographic data. Quantification was based on a series of calibrators ranging from 0.031 to 32 µg/mL, prepared by adding test compound to drug free rat plasma. Quality control samples were analyzed in parallel to verify that the system performs in control.

6.2.5 Statistics

Data from whole blood assay, paw edema and SCW models were analysed using Graph Pad Prism software. Difference between treatment groups as well as difference between treatment groups and control were compared using ANOVA followed by Dunnet's test.

Pharmacokinetic parameters namely - maximum plasma concentration (C_{max}), time point of maximum plasma concentration (t_{max}), area under the plasma concentration - time curve from 0 hour to infinity ($AUC_{0-\infty}$) and half-life of drug elimination during the terminal phase ($t_{1/2}$) were calculated from plasma

concentration versus time data, by standard non-compartmental methods, using the WinNonLin software version 4.0.1 procured from Pharsight Corporation, USA.

7 References:

1. Ferrero-Miliani L., Nielsen O.H., Andersen P.S., Girardin S.E., Chronic inflammation: importance of NOD2 and NALP3 in interleukin-1β generation, *Clin. Exp.Immunol.*, **2007**, 147: 227–235.

2. EiroN., Vizoso F.J., Inflammation and cancer, *World J of Gastrointestinal Surg.*, **2012**, 4: 62–72.

3. Lee Y.W., Kim P.H., Won H. L., Hirani A.A., Interleukin-4, oxidative stress, vascular inflammation and atherosclerosis, *Biomol. And Therap.*, **2010**, 18:135–144.

4. Wyss-Coray T., Rogers J., Inflammation in Alzheimer disease-a brief review of the basic science and clinical literature, *Cold Spring Harb Perspect Med,* **2012**, 2: 1-20.

5. Urrutia P., Aguirre P., Esparza A., Tapia V., Mena N.P., Arredondo M, González-Billault C, Núñez M.T., Inflammation alters the expression of DMT1, FPN1 and hepcidin, and it causes iron accumulation in central nervous system cells, *J of Neurochem.*, **2013**, 126: 541–549.

6. Wee Yong V., Inflammation in neurological disorders: a help or a hindrance? *Neuroscientist*, **2010**, 16: 408–420.

7. Provinciali M., Cardelli M., Marchegiani F., Inflammation, chronic obstructive pulmonary disease and aging, *Current Opinion in Pulmon. Med*, **2011**, 17 (suppl. 1): S3–S10.

8. O'Rourke S.M., Herskowitz I., The Hog1 MAPK prevents cross talk between the HOG and pheromone response MAPK pathways in Saccharomyces cerevisiae, *Genes and Development*, **1998**, 12: 2874–2886.

9. Lee J.C., Laydon J.T., McDonnell P.C., A protein kinase involved in the regulation of inflammatory cytokine biosynthesis, *Nature*, **1994**, 372: 739–746.

10. Huh J.E., Jung I.T., Choi J., The natural flavonoid galangin inhibits osteoclastic bone destruction and osteoclastogenesis by suppressing NF-kappa ß in collagen-induced arthritis and bone marrow-derived macrophages, *Eur. J of Pharmacol.*, **2013**, 698: 57–66.

11. Kim M., Li Y.X., Dewapriya P., Ryu B., Kim S.K., Floridoside suppresses pro-inflammatory responses by blocking MAPK signaling in activated microglia, *BMB Reports*, **2013**, 46: 398–403.

12. Schieven G.L., The biology of p38 kinase: a central role in inflammation, *Current Topics in Med. Chem.*, **2005**, 5: 921–928.

13. Rajashekhar G, Kamocka M, Marin A, Suckow M.A., Wolter W.R., Badve S., Pro-inflammatory angiogenesis is mediated by p38 MAP kinase, *J of Cellular Physiol.*, **2011**, 226: 800–808.

14. Clark A.R., Dean J.L., The p38 MAPK pathway in rheumatoid arthritis: a sideways look, *The Open Rheumatol. J*, **2012**, 6: 209–219.

15. Ren F, Zhang H.Y., Piao Z.F., Zheng S.J., Chen Y, Chen D.X., Duan Z.P., Inhibition of glycogen synthase kinase 3b activity regulates Toll-like receptor 4-mediated liver inflammation, *ZhonghuaGanZang Bing ZaZhi*, **2012**, 20: 693–697.

16. Limand A.K., Tesch G.H., Inflammation in diabetic nephropathy, *Mediators of Inflammation*, **2012**, Article ID 146154, 12 pages.

17. Ko H.M., Joo S.H., Kim P, Park J.H., Kim H.J., Bahn G.H., Kim H.Y., Lee J, Han S.H., Shin C.Y., Park S.H., Effects of Korean red ginseng extract on tissue plasminogen activator and plasminogen activatorinhibitor-1 expression in cultured rat primary astrocytes, *Journal of Ginseng Research,* **2013**, 37: 401–412.

18. Yang Y, Kim S.C., Yu T, Yi Y.S., Rhee M.H., Sung G.H, Yoo B.C., Cho J.Y., Functional Roles of p38 mitogen-activated protein kinase in macrophage-mediated inflammatory responses, *Mediators of Inflammation*, **2014**, 2014, Article ID 352371, 13 pages.

19. Jiang Y., Chen C., Li Z., Characterization of the structure and function of a new mitogen-activated protein kinase (p38β), *J of Biol. Chem.*, **1996**, 271: 17920–17926.

20. Li Z., Jiang Y., Ulevitch R.J., Han J., The primary structure of p38γ: a new member of p38 group of MAP kinases, *Biochem. Biophys. Res. Comm.*, **1996**, 228: 334–340.

21. Hale K.K., Trollinger D., Rihanek M., Manthey C.L., Differential expression and activation of p38 mitogen-activated protein kinase α, β, γ, and δ in inflammatory cell lineages, *J Immunol.*, **1999**, 162: 4246–4252.

22. Nick A., Avdi N.J., Gerwins P., Johnson G.L., Worthen G.S., Activation of a p38 mitogen-activated protein kinase in human neutrophils by lipopolysaccharide, *J Immunol.*, **1996**, 156:4867–4875.

23. Shapiro L., Puren A.J., Barton H.A. Interleukin 18 stimulates HIV type 1 in monocytic cells, *PNAS*, **1998**, 95: 12550–12555.

24. Keesler G.A., Bray J., Hunt J., Johnson D.A., Gleason T, Yao Z, Wang S., Parker C., Yamane H., Cole C., Lichenstein H. S., Purification and activation of recombinant p38 isoforms α, β, γ and δ, *Protein Exp. Purif.*, **1998**, 14: 221–228.

25. Jiang Y, Gram H, Zhao M, New L, Gu J, Feng L, Padova F.D., Ulevitch R.J., Han J, Characterization of the structure and function of the fourth member of p38 group mitogen-activated protein kinases, p38δ, *J Biol. Chem.*, **1997**, 272: 30122–30128.

26. Lee J.C., Laydon J.T., McDonnell P.C., Gallagher T.F., Kumar S, Green D, McNulty D, Blumenthal M.J., Heys J.R., Landvatter S.W., A protein kinase involved in the regulation of inflammatory cytokine biosynthesis, *Nature,* **1994**, 372: 739–746.

27. Badger A.M., Bradbeer J.N., Votta B, Lee J.C., Adams J.L., Griswold D.E., Pharmacological profile of SB, 203580, a selective inhibitor of cytokine suppressive binding protein/p38 kinase in animal models of arthritis, bone resorption, endotoxin shock and immune function. *J. Pharmacol. Exp. Ther.*, **1996**, 279: 1453–1461.

28. Capdeville R., Buchdunger E, Zimmermann J, Matter A., Glivec (STI571, imatinib), a rationally developed, targeted anticancer drug. *Nat. Rev. Drug Discov.*, **2002**, 1: 493–502.

29. Jackson P.F., Bullington J.L., Pyridinyl imidazole basedp38 MAP kinase inhibitors. *Curr. Top. Med. Chem,* **2002**, 2: 1011–1020.

30. Hynes J., Leftheris K., Small molecule p38 inhibitors: novel structure features and advances from 2002–2005. *Curr. Top. Med. Chem.,* **2005**, 5: 967–985.

31. Goldstein D.M., Gabriel T., Pathway to the clinic: inhibition of p38 MAP kinase. A review of ten chemotypes selected for development. *Curr. Top. Med. Chem.,* **2005,** 5: 1017–1029.

32. Wrobleski S.T., Doweyko A.M., Structural comparison of p38 inhibitor–protein complexes: a review of recent p38 inhibitors having unique binding interactions. *Curr. Top. Med. Chem.,* **2005,** 5: 1005–1016.

33. Zhang J, Shen B,Lin A, Novel strategies for inhibition of thep38 MAPK pathway, *Trends Pharmacol. Sci.,* **2007**, 28: 286-295.

34. Koeberle S.C., Fischer S, Schollmeyer D, Schattel V, Rauh C.D., Laufer S.A., Design, synthesis, and biological evaluation of novel disubstituted dibenzosuberones as highly potent and selective inhibitors of p38 mitogen activated protein kinase, *J. Med. Chem.,* **2012**, 55: 5868-5877.

35. Fischer S., Koeberle S.C., Laufer S.A., p38α mitogen-activated protein kinase inhibitors, a patent review (2005-2011)., *Expert Opin. Ther. Pat.,* **2011**, 21:1843-1866.

36. Karcher S.C., Laufer S.A., Successful structure-based design of recent p38 MAP kinase inhibitors, *Curr. Top.Med. Chem.,* **2009**, 9: 655–676.

37. Miwatashi S, Arikawa Y, Kotani E, Miyamoto M, Naruo K, Kimura H, Tanaka T, Asahi S, Ohkawa S, Novel inhibitor of p38 MAP kinase as an anti-TNF-α drug: discovery of N-[4-[2-Ethyl-4-(3-methylphenyl)-1,3-thiazol-5-yl]-2-pyridyl]benzamide (TAK-715) as a potent and orally active anti-rheumatoid arthritis agent, *J. Med. Chem.*, **2005**, 48: 5966-5979.

38. Beletskaya I.P, Cheprakov A.V., Copper in cross-coupling reactions: The post-Ullmann chemistry, *Coordination Chemistry Reviews*, **2004**, 248: 2337-2364.

39. Sedelmeier J, Bolm C, Efficient Copper-catalyzed N-arylation of sulfoximines with aryl iodides and aryl bromides, *J. Org. Chem.*, **2005**, 70: 6904-6906.

40. Johnson C.R., Haake M., Schroeck C.W., Chemistry of sulfoxides and related compounds. XXVI. Preparation and synthetic applications of (dimethylamino)phenyl oxosulfoniummethylide, *J. Am. Chem. Soc.* **1970**, 92: 6594-6598.

41. Yadav M.R., Rit R.K., Sahoo A.K., Sulfoximines: A reusable directing group for chemo- and regioselective ortho CH oxidation of arenes, *Chem. Eur. J*, **2012**, 18: 5541-5545.

Characterization Data

4-(2-ethyl-4-(4-fluorophenyl)thiazol-5-yl)pyridin-2-amine (6)

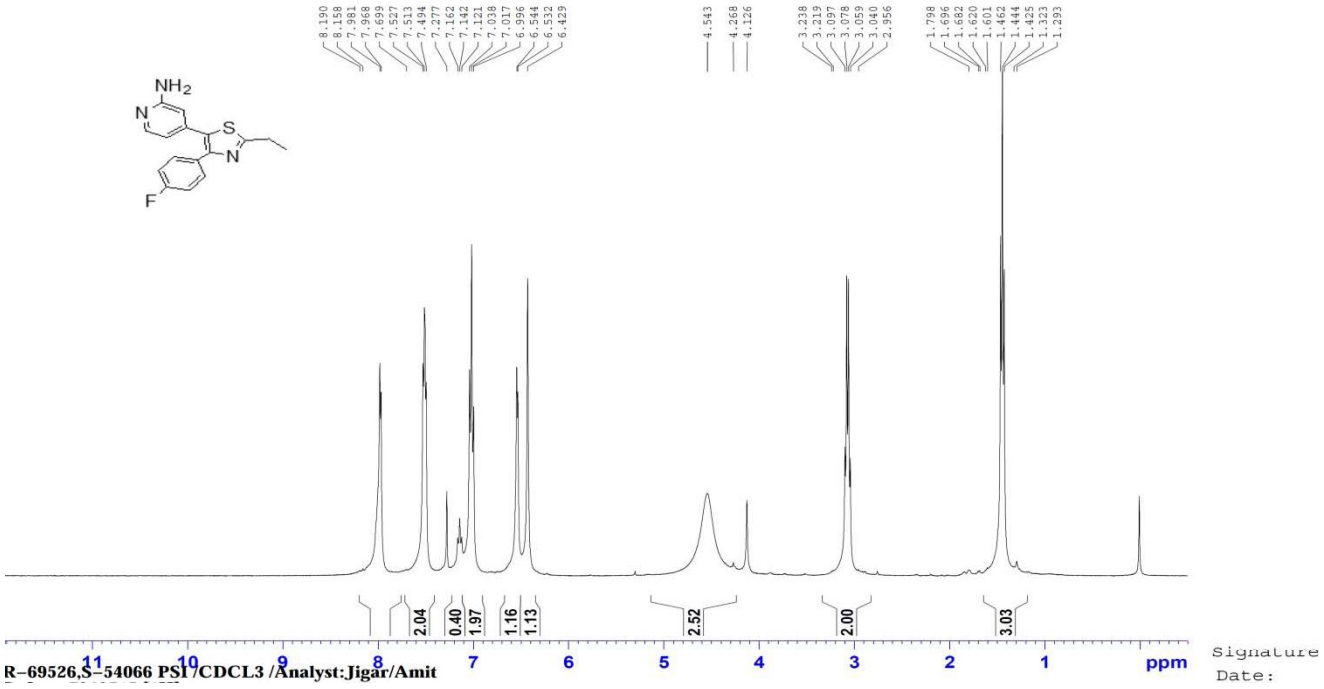
8.190
8.158
7.981
7.968
7.699
7.527
7.513
7.494
7.277
7.162
7.142
7.121
7.038
7.017
6.996
6.544
6.532
6.429
4.543
4.268
4.126
3.238
3.219
3.097
3.078
3.059
3.040
2.956
1.798
1.696
1.682
1.620
1.601
1.462
1.444
1.425
1.323
1.293
NH2
N
S
N
F
2.04
0.40
1.97
1.16
1.13
2.52
2.00
3.03
11
10
9
8
7
6
5
4
3
2
1
ppm
R-69526,S-54066 PSI7/CDCL3 /Analyst:Jigar/Amit
Signature
Date:

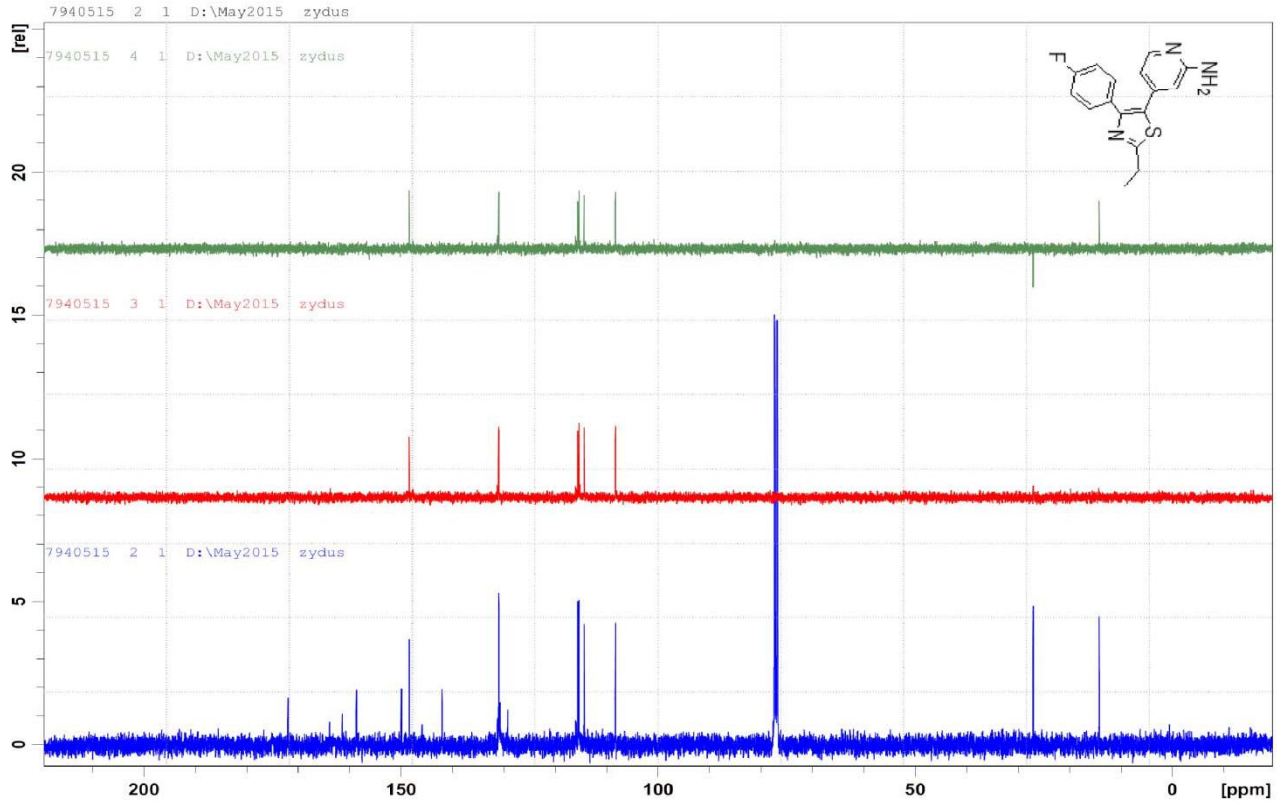
7940515 2 1 D:\May2015 zydus
7940515 4 1 D:\May2015 zydus
7940515 3 1 D:\May2015 zydus
7940515 2 1 D:\May2015 zydus
[rel]
20
15
10
5
0
200
150
100
50
0
[ppm]
F
N
NH2
S
N

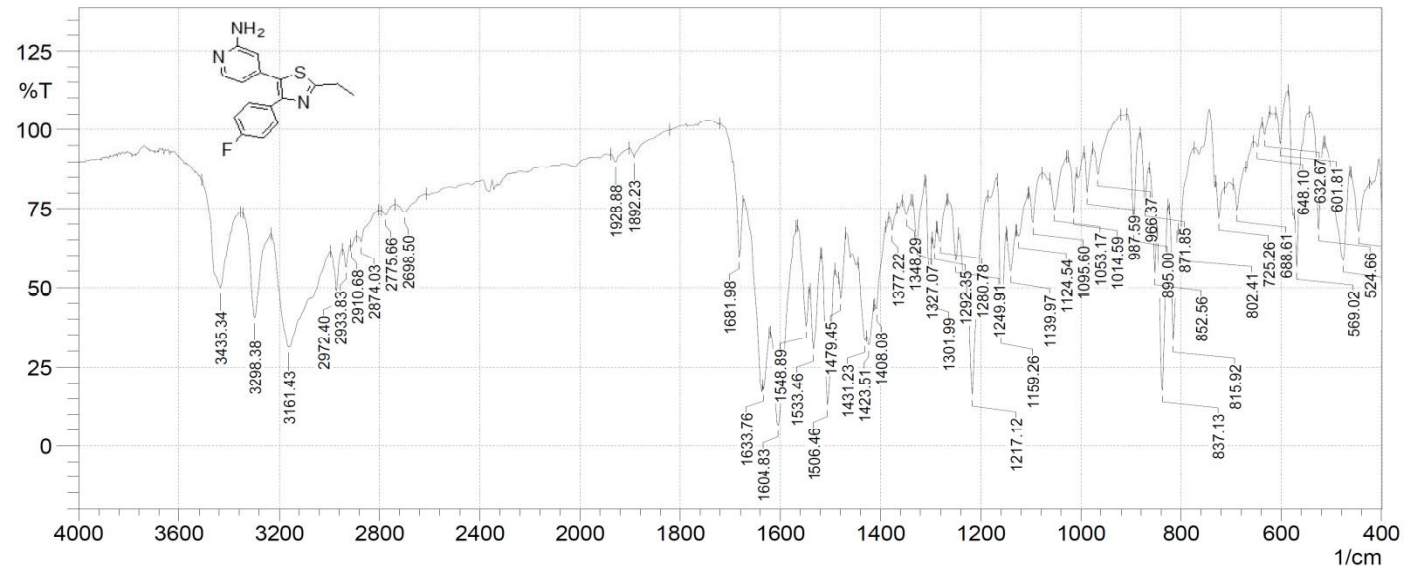
%T
1/cm
3435.34
3298.38
3161.43
2972.40
2933.83
2910.68
2874.03
2775.66
2698.50
1928.88
1892.23
1681.98
1633.76
1604.83
1548.89
1533.46
1506.46
1479.45
1431.23
1423.51
1408.08
1377.22
1348.29
1327.07
1301.99
1292.35
1280.78
1249.91
1217.12
1159.26
1139.97
1124.54
1095.60
1053.17
1014.59
987.59
966.37
895.00
871.85
852.56
837.13
815.92
802.41
725.26
688.61
648.10
632.67
601.81
569.02
524.66

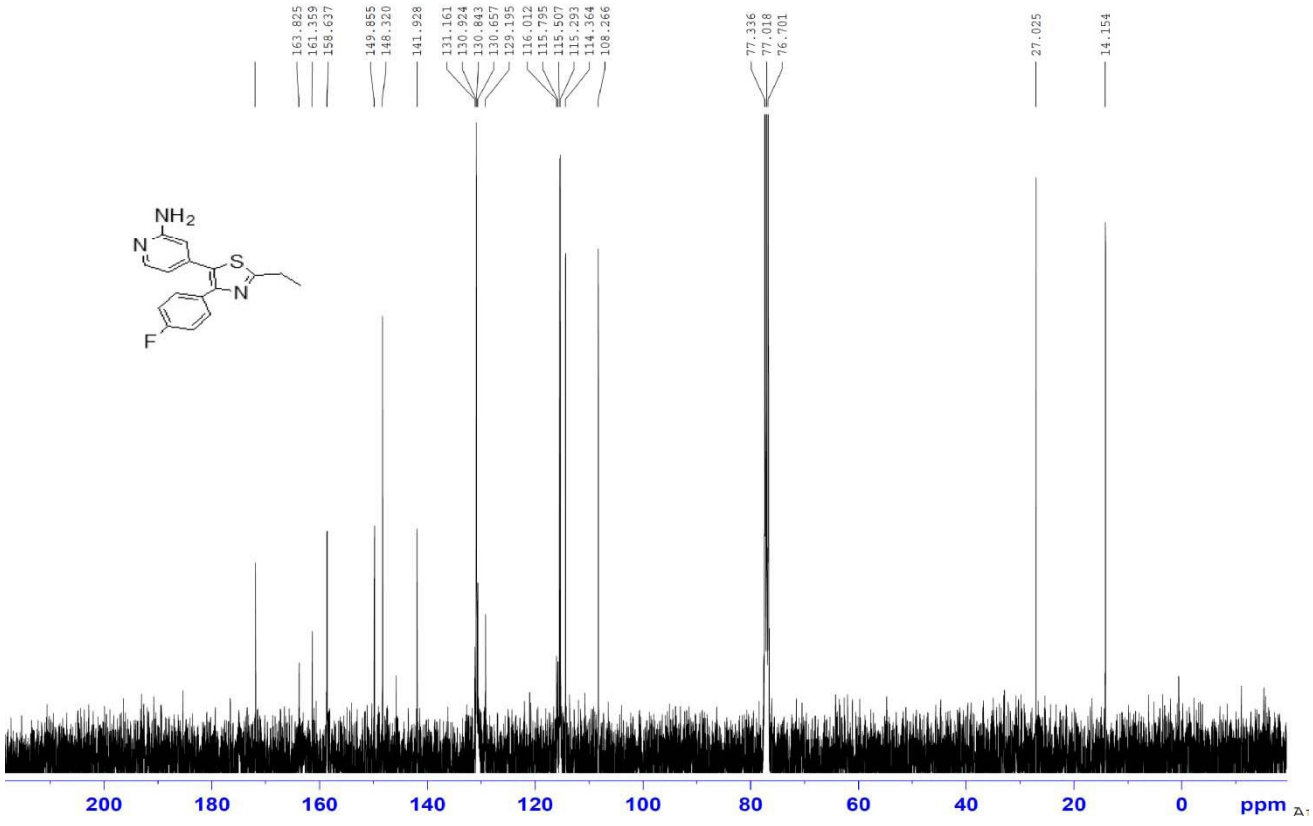
163.825
161.359
158.637
149.855
148.320
141.928
131.161
130.924
130.843
130.657
129.195
116.012
115.795
115.507
115.293
114.364
108.266
77.336
77.018
76.701
27.025
14.154
ppm

4-[2-ethyl-4-(4-fluoro-phenyl)-thiazol-5-yl]-2-iodo- pyridine (8)

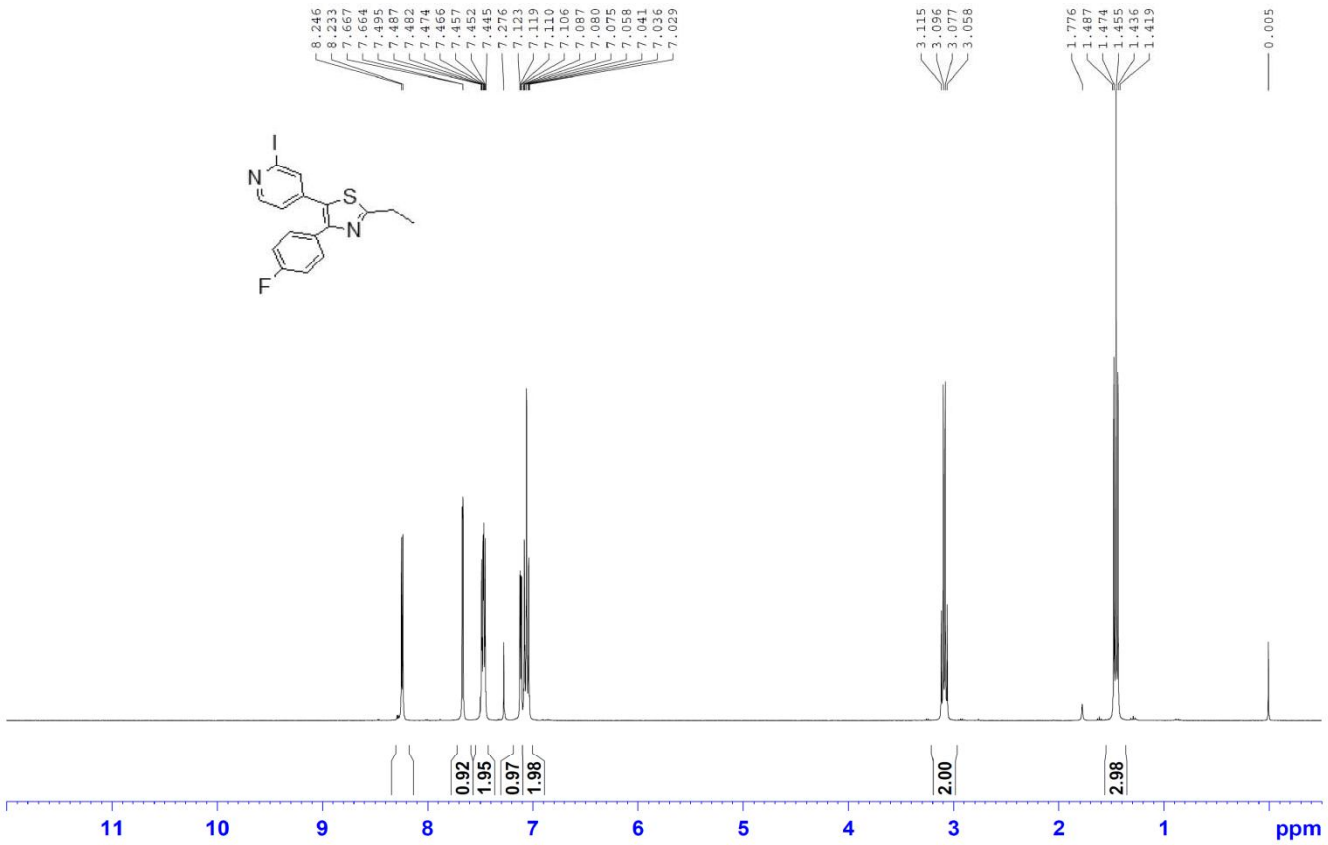
8.246
8.233
7.667
7.664
7.495
7.487
7.482
7.474
7.466
7.457
7.452
7.445
7.276
7.123
7.119
7.110
7.106
7.087
7.080
7.075
7.058
7.041
7.036
7.029
3.115
3.096
3.077
3.058
1.776
1.487
1.474
1.455
1.436
1.419
0.005
I
N
S
N
F
0.92
1.95
0.97
1.98
2.00
2.98
11
10
9
8
7
6
5
4
3
2
1
ppm

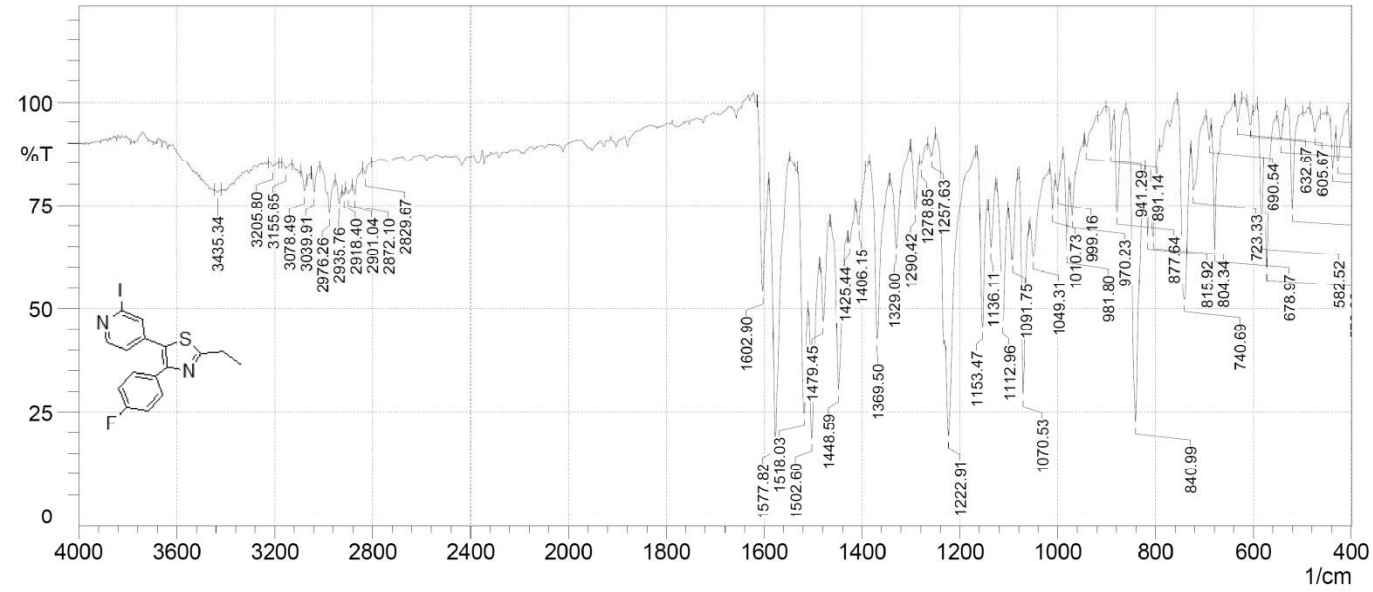
100
%T
75
50
25
0
3435.34
3205.80
3155.65
3078.49
3039.91
2976.26
2935.76
2918.40
2901.04
2872.10
2829.67
1602.90
1577.82
1518.03
1502.60
1479.45
1448.59
1425.44
1406.15
1369.50
1329.00
1290.42
1278.85
1257.63
1222.91
1153.47
1136.11
1112.96
1091.75
1070.53
1049.31
1010.73
999.16
981.80
970.23
941.29
891.14
877.64
840.99
815.92
804.34
740.69
723.33
690.54
678.97
632.67
605.67
582.52
I
N
S
N
F
4000
3600
3200
2800
2400
2000
1800
1600
1400
1200
1000
800
600
400
1/cm

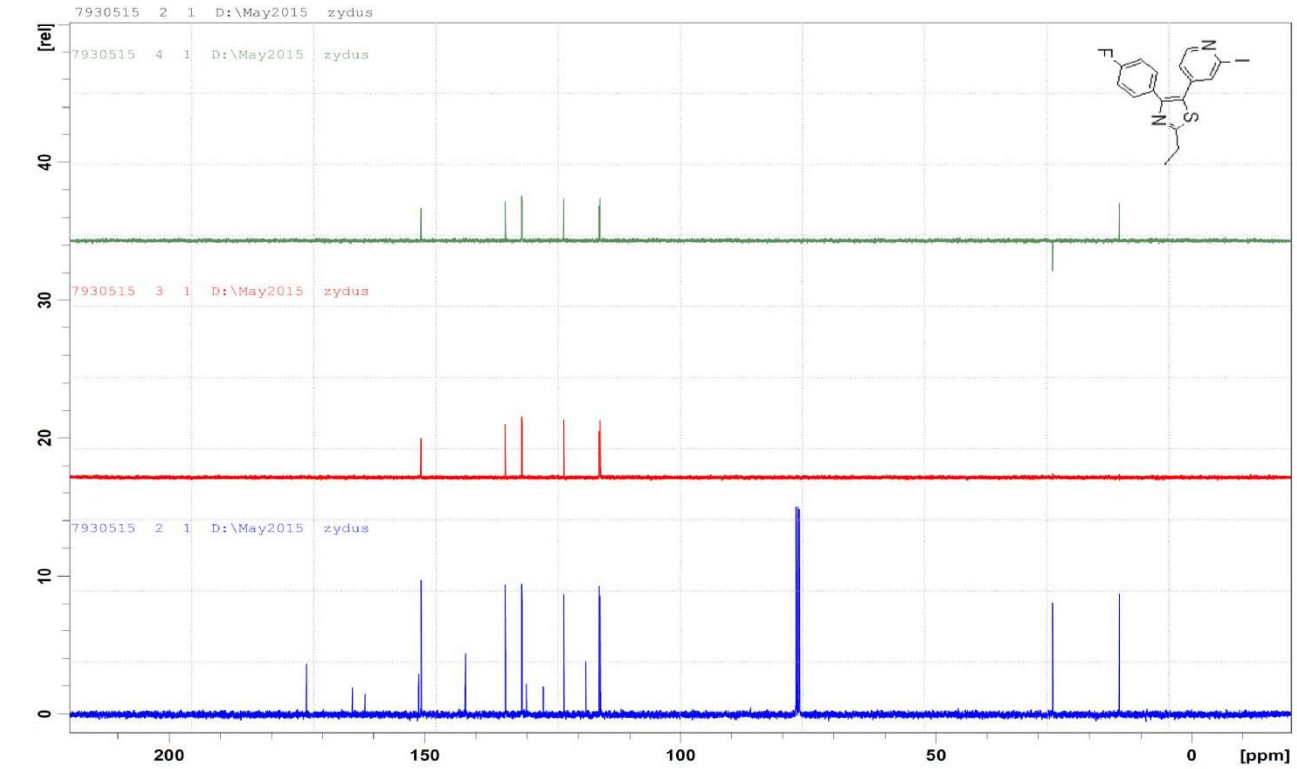
7930515 2 1 D:\May2015 zydus
7930515 4 1 D:\May2015 zydus
7930515 3 1 D:\May2015 zydus
7930515 2 1 D:\May2015 zydus
[rel]
0
10
20
30
40
200
150
100
50
0
[ppm]

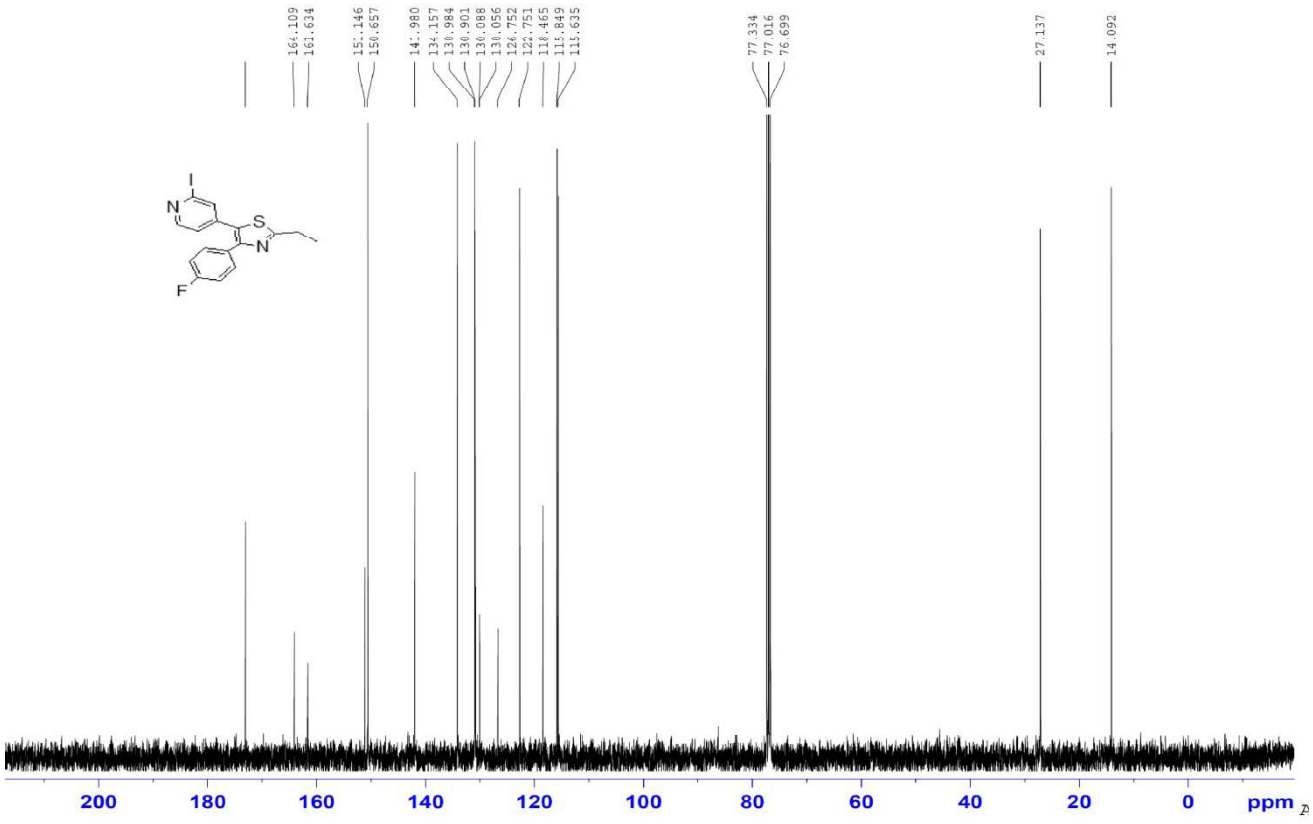
164.109
161.634
151.146
150.657
141.980
134.157
130.984
130.901
130.088
130.056
126.752
122.751
118.465
115.849
115.635
77.334
77.016
76.699
27.137
14.092
200
180
160
140
120
100
80
60
40
20
0
ppm

Intermediate Sulfoximine

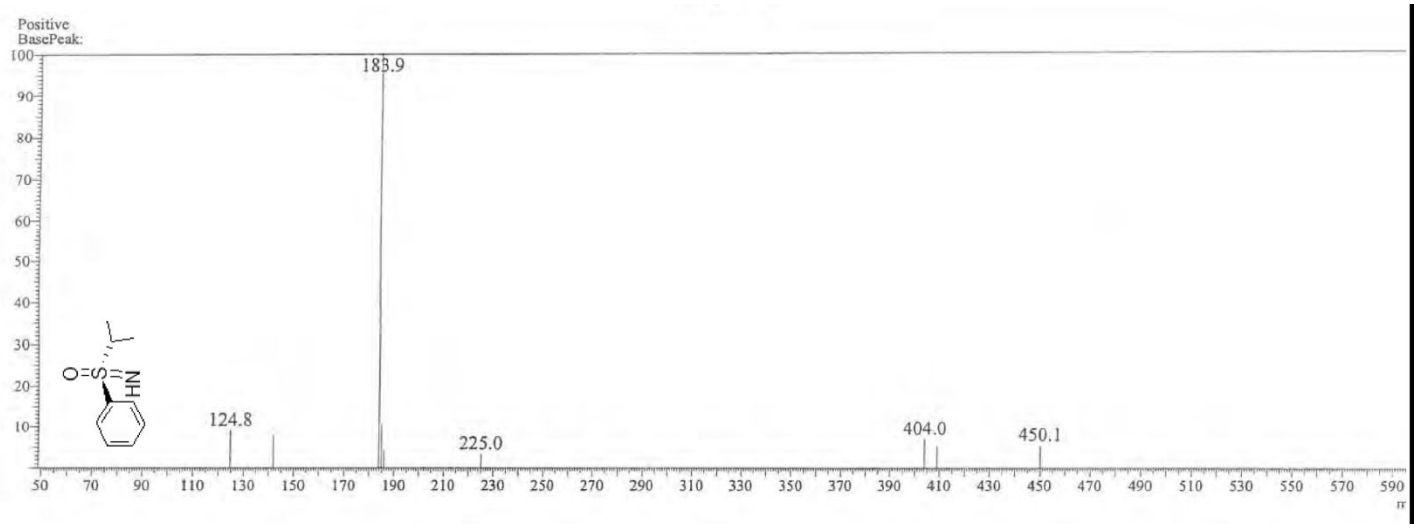

SAMPLE INFORMATION

Sample Name:	KB-INT-A	Acquired By:	UPLC
Sample Type:	Unknown	Sample Set Name:	AUG0112
Vial:	1:D,4	Acq. Method Set:	MEDCHEM_G1
Injection #:	1	Processing Method:	Default
Injection Volume:	1.00 ul	Channel Name:	blank_0108125
Run Time:	9.0 Minutes	Proc. Chnl. Descr.:	[ACQUITY TUV ChA] - Labeled:
Flow : 0.4 ml/min		Date Acquired:	8/1/2012 7:51:57 PM IST
MobilePhase : 0.05% TFA in Water:ACN (Gradient)		Date Processed:	8/3/2012 10:33:52 AM IST
Column_Type : BEH C18 (2.1X100 mm)1.7u			

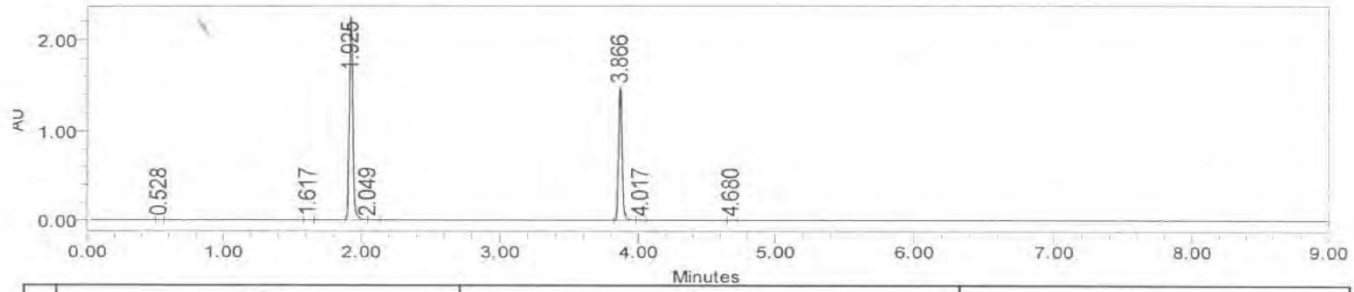

	RT	Area	% Area
1	0.528	3337	0.05
2	1.617	5293	0.08
3	1.925	3961456	59.87
4	2.049	5927	0.09
5	3.866	2631517	39.77
6	4.017	7340	0.11
7	4.680	2356	0.04

Compound (1)

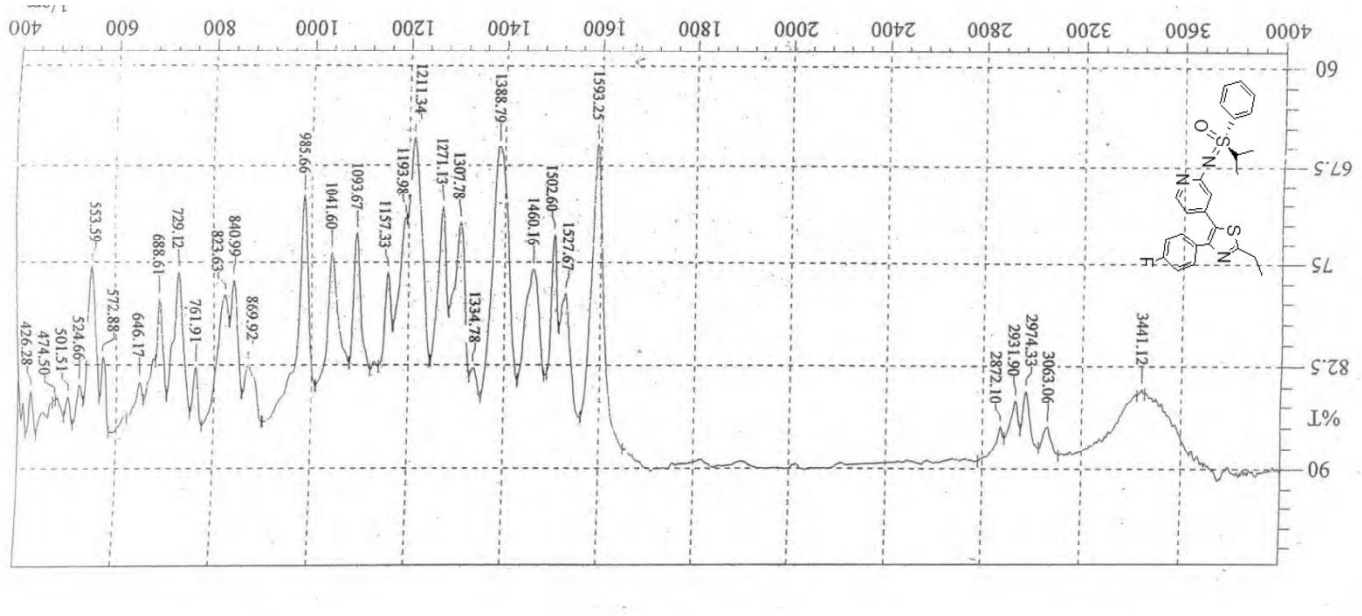

Mass Spectrum

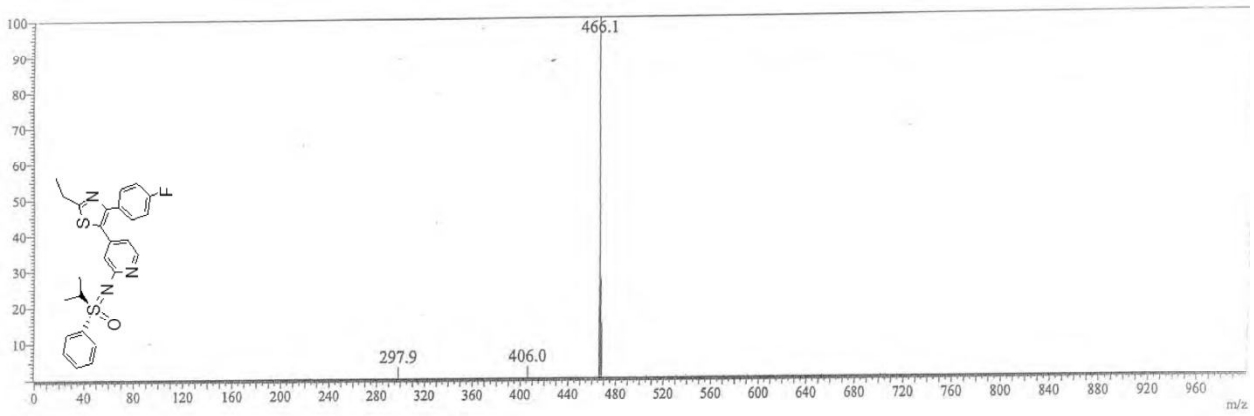

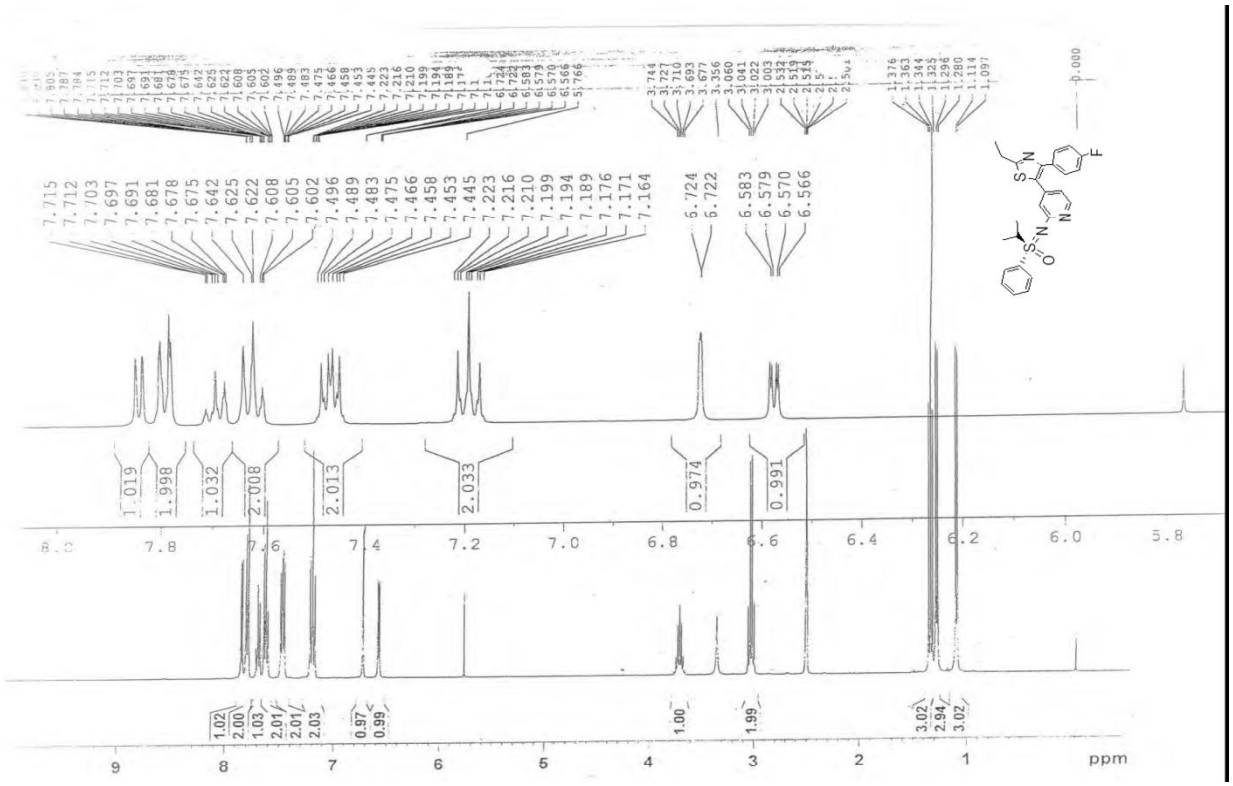
7.715
7.712
7.703
7.697
7.691
7.681
7.678
7.675
7.642
7.625
7.622
7.608
7.605
7.602
7.496
7.489
7.483
7.475
7.466
7.458
7.453
7.445
7.223
7.216
7.210
7.199
7.194
7.189
7.176
7.171
7.164
6.724
6.722
6.583
6.579
6.570
6.566
1.019
1.998
1.032
2.008
2.013
2.033
0.974
0.991
8.0
7.8
7.6
7.4
7.2
7.0
6.8
6.6
6.4
6.2
6.0
5.8
1.02
2.00
1.03
2.01
2.01
2.03
0.97
0.99
1.00
1.99
3.02
2.94
3.02
9
8
7
6
5
4
3
2
1
ppm

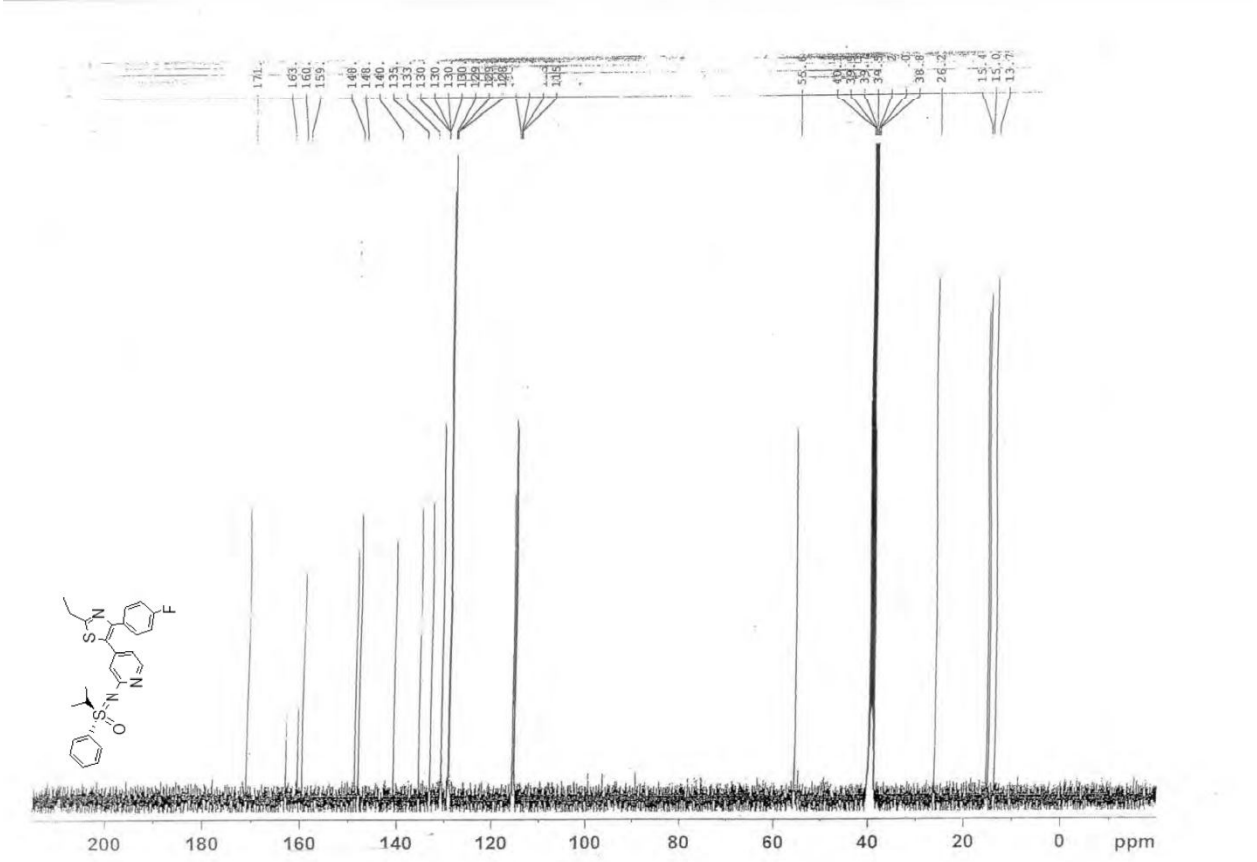
200
180
160
140
120
100
80
60
40
20
0
ppm

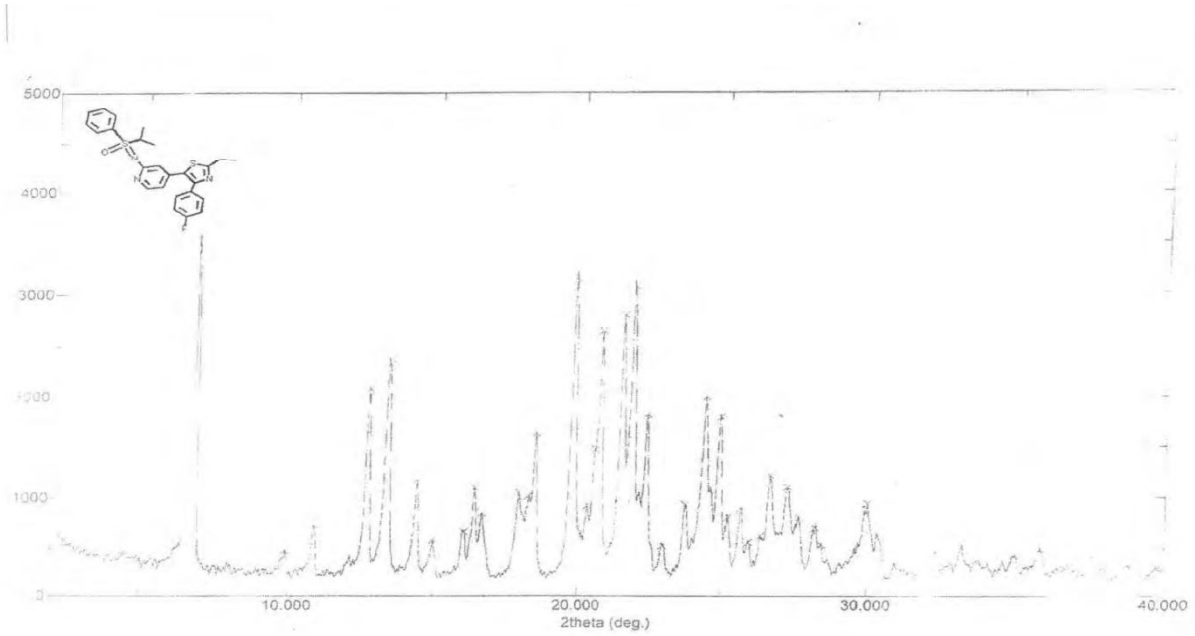
5000
4000
3000
1000
0
10.000
20.000
30.000
40.000
2theta (deg.)

HCl salt of Compound (1)

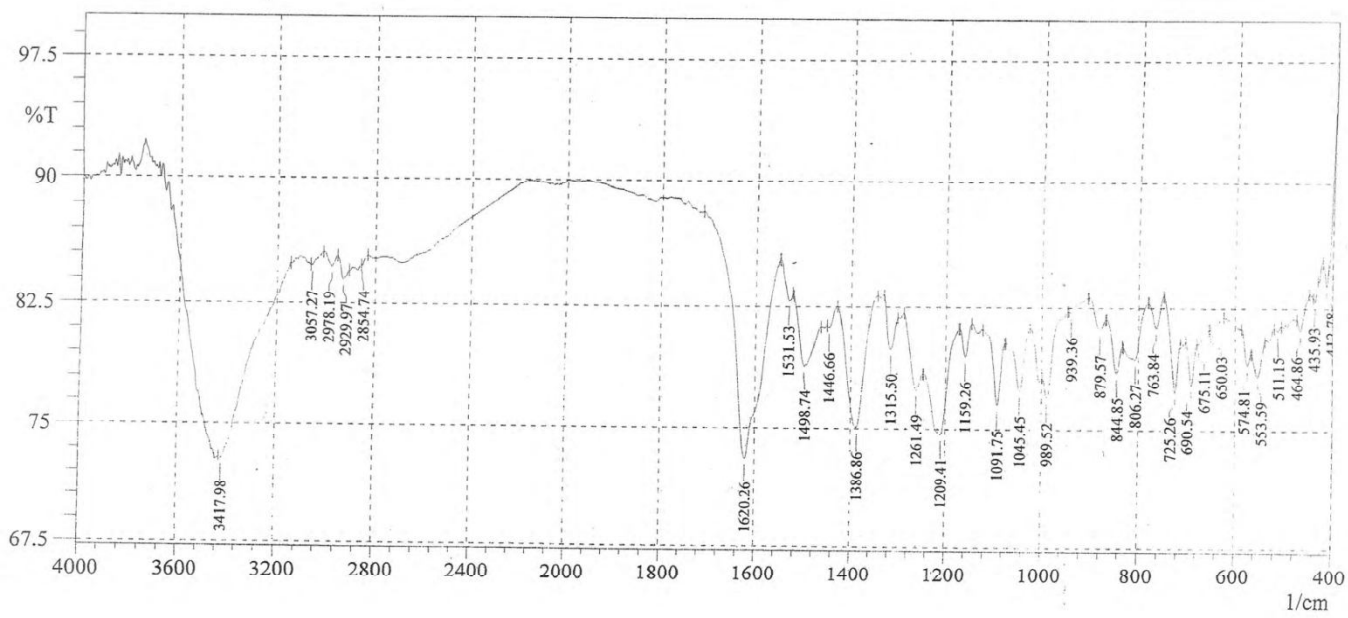
97.5
%T
90
82.5
75
67.5
4000
3600
3200
2800
2400
2000
1800
1600
1400
1200
1000
800
600
400
1/cm
3417.98
3057.27
2978.19
2929.97
2854.74
1620.26
1531.53
1498.74
1446.66
1386.86
1315.50
1261.49
1209.41
1159.26
1091.75
1045.45
989.52
939.36
879.57
844.85
806.27
763.84
725.26
690.54
675.11
650.03
574.81
553.59
511.15
464.86
435.93

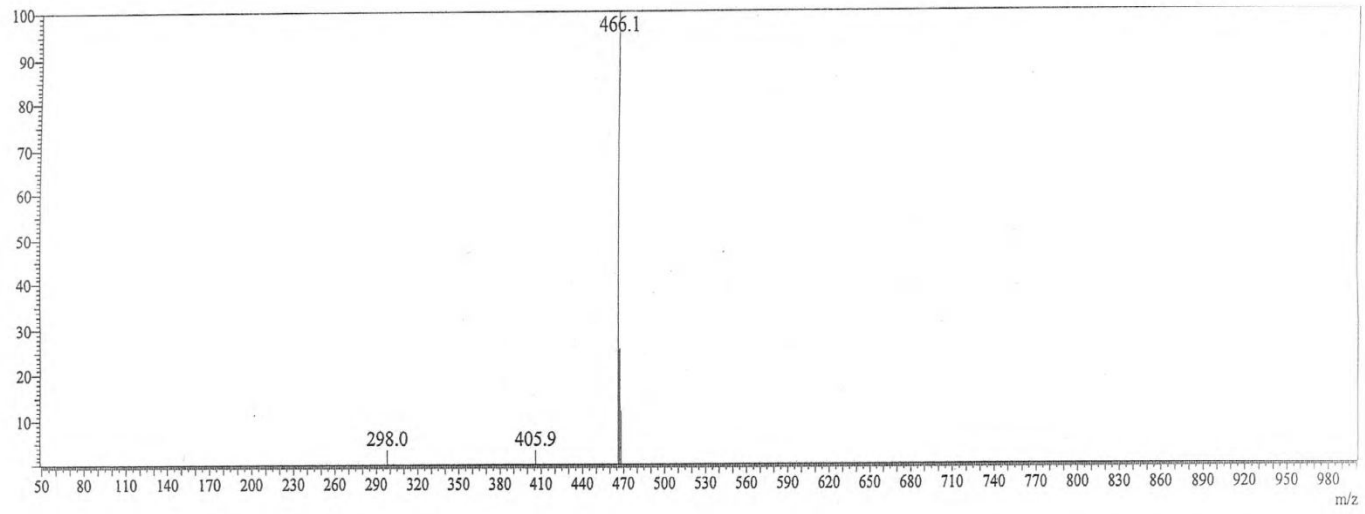
100
90
80
70
60
50
40
30
20
10
466.1
298.0
405.9
50
80
110
140
170
200
230
260
290
320
350
380
410
440
470
500
530
560
590
620
650
680
710
740
770
800
830
860
890
920
950
980
m/z

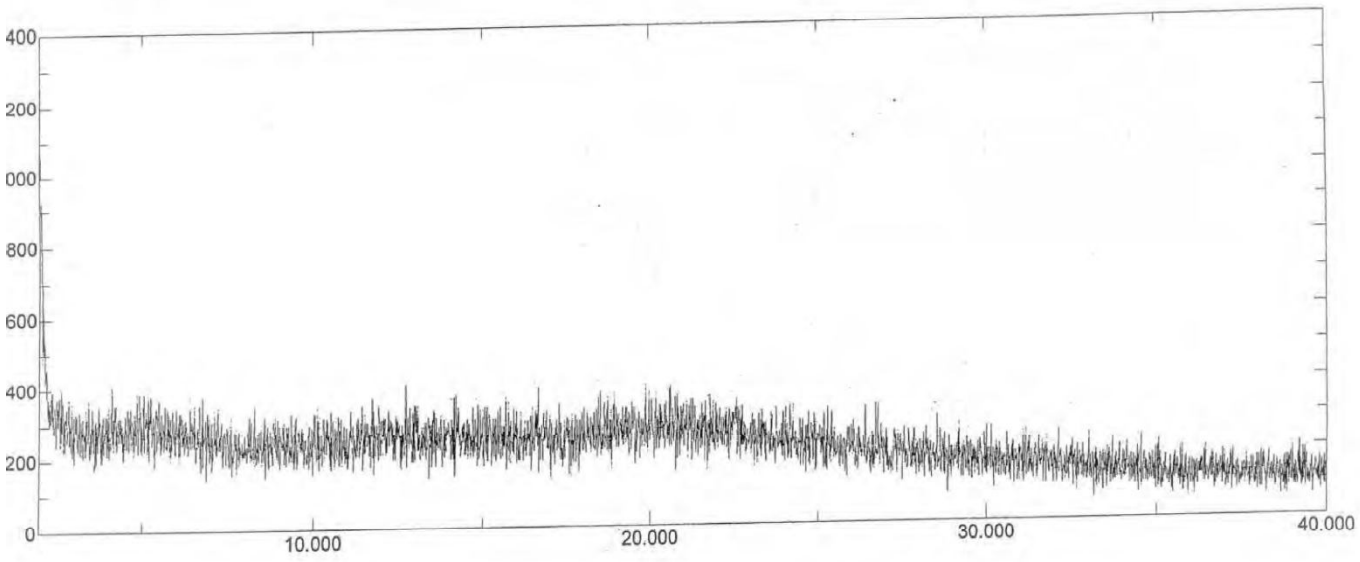
400
200
000
800
600
400
200
0
10.000
20.000
30.000
40.000

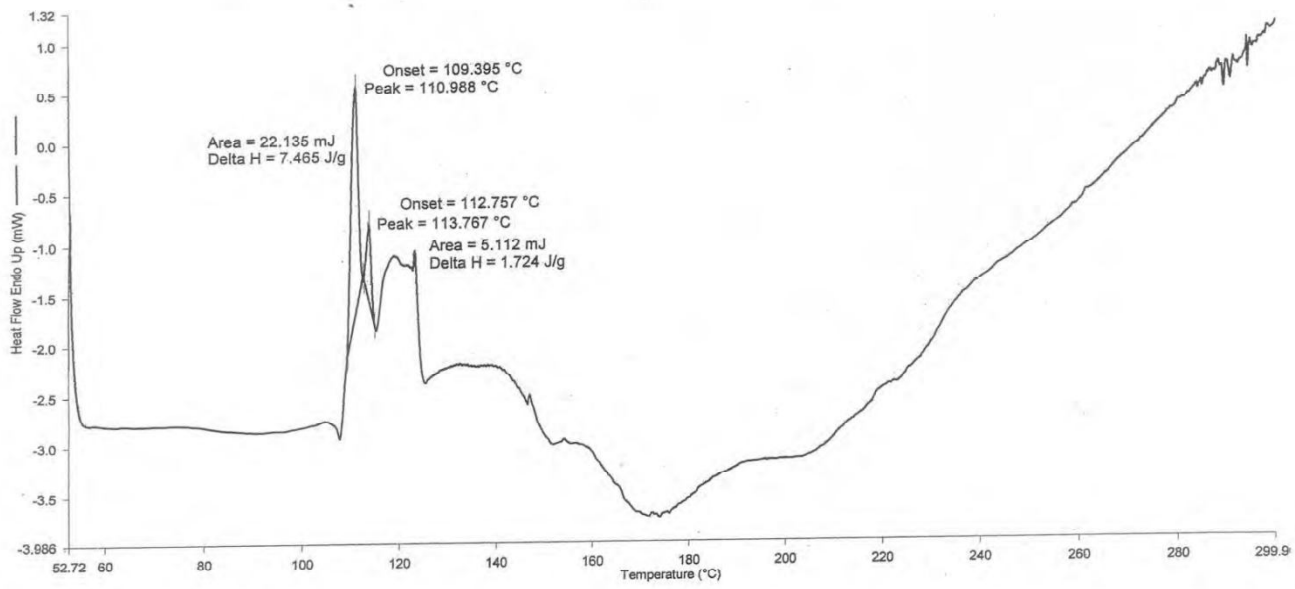
Onset = 109.395 °C
Peak = 110.988 °C
Area = 22.135 mJ
Delta H = 7.465 J/g
Onset = 112.757 °C
Peak = 113.767 °C
Area = 5.112 mJ
Delta H = 1.724 J/g
Heat Flow Endo Up (mW)
Temperature (°C)
1.32
1.0
0.5
0.0
-0.5
-1.0
-1.5
-2.0
-2.5
-3.0
-3.5
-3.986
52.72
60
80
100
120
140
160
180
200
220
240
260
280
299.9

PTSA salt of compound (1)

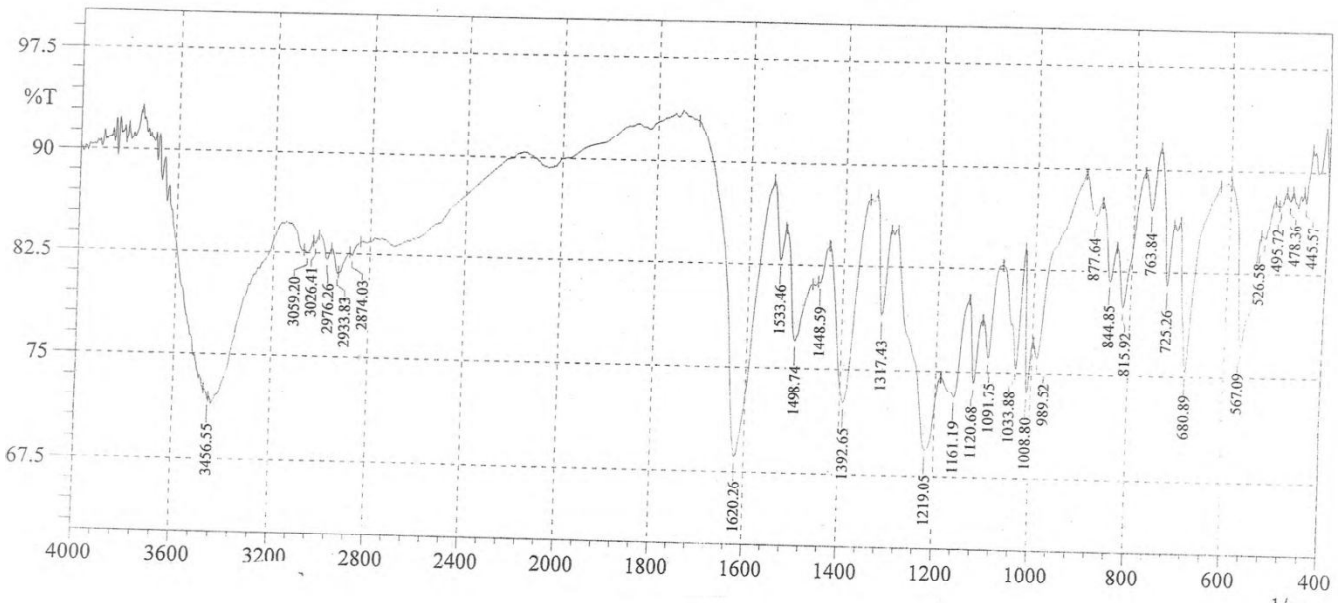
97.5
%T
90
82.5
75
67.5
3456.55
3059.20
3026.41
2976.26
2933.83
2874.03
1620.26
1533.46
1498.74
1448.59
1392.65
1317.43
1219.05
1161.19
1120.68
1091.75
1033.88
1008.80
989.52
877.64
844.85
815.92
763.84
725.26
680.89
567.09
526.58
495.72
478.36
445.57
4000
3600
3200
2800
2400
2000
1800
1600
1400
1200
1000
800
600
400

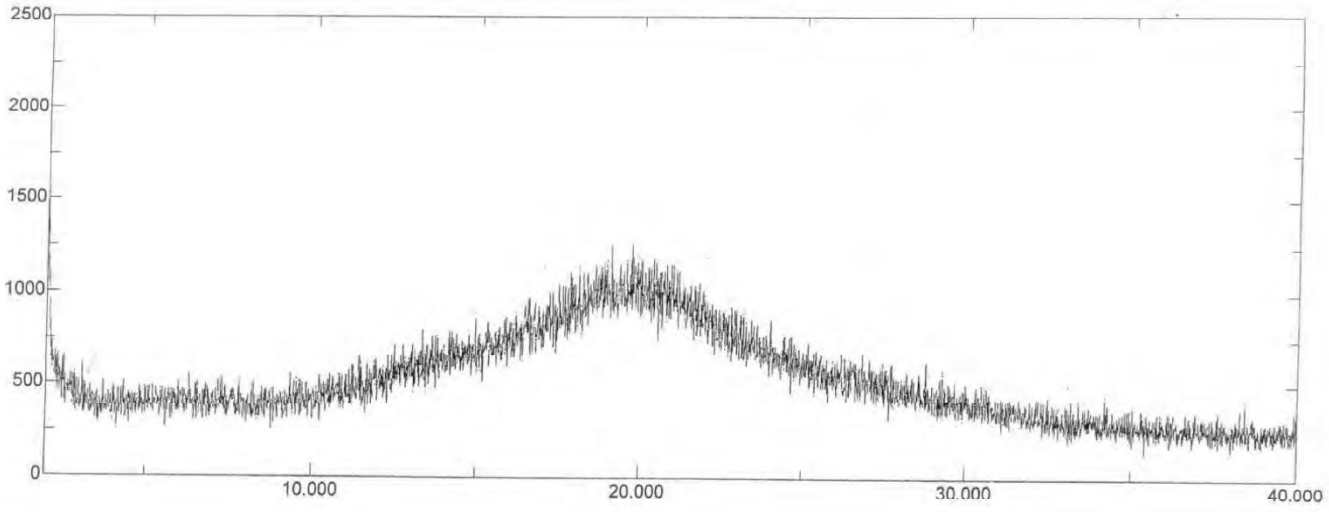
2500
2000
1500
1000
500
0
10.000
20.000
30.000
40.000

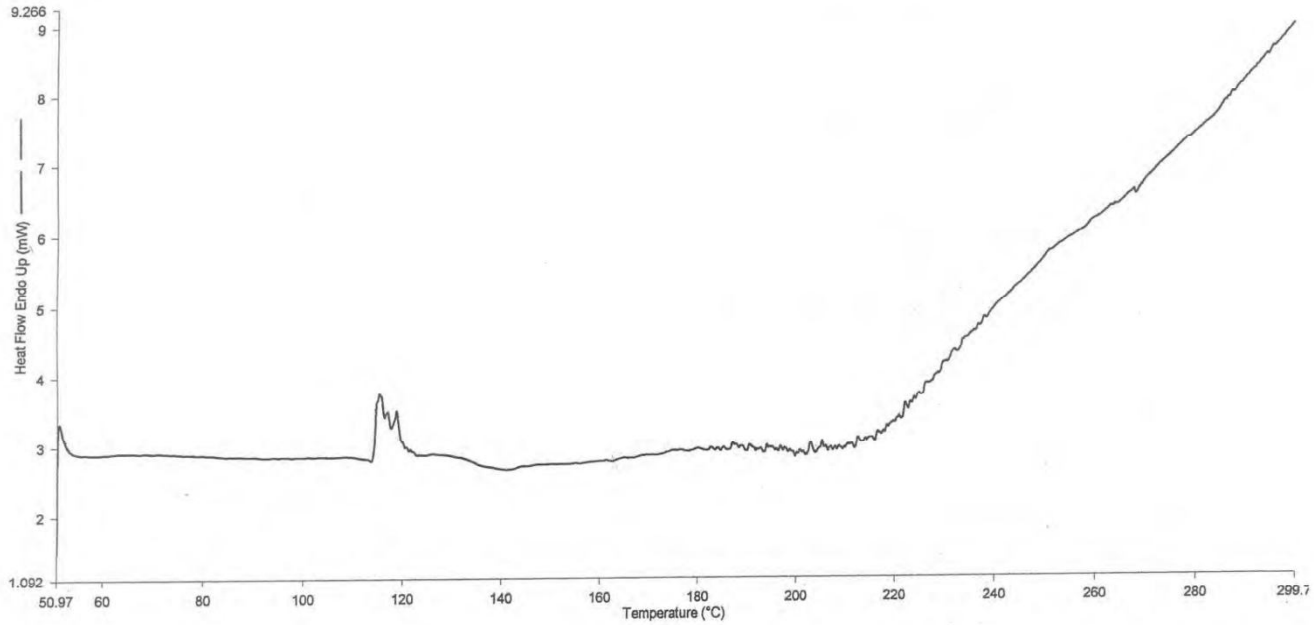

Mass Spectrum

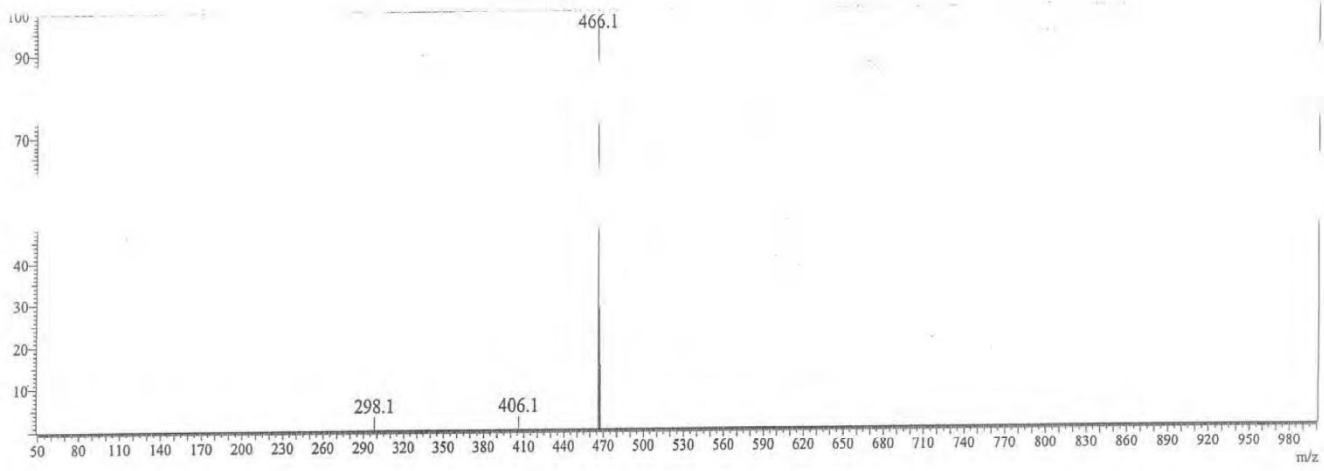

Bisulfate salt of compound (1)

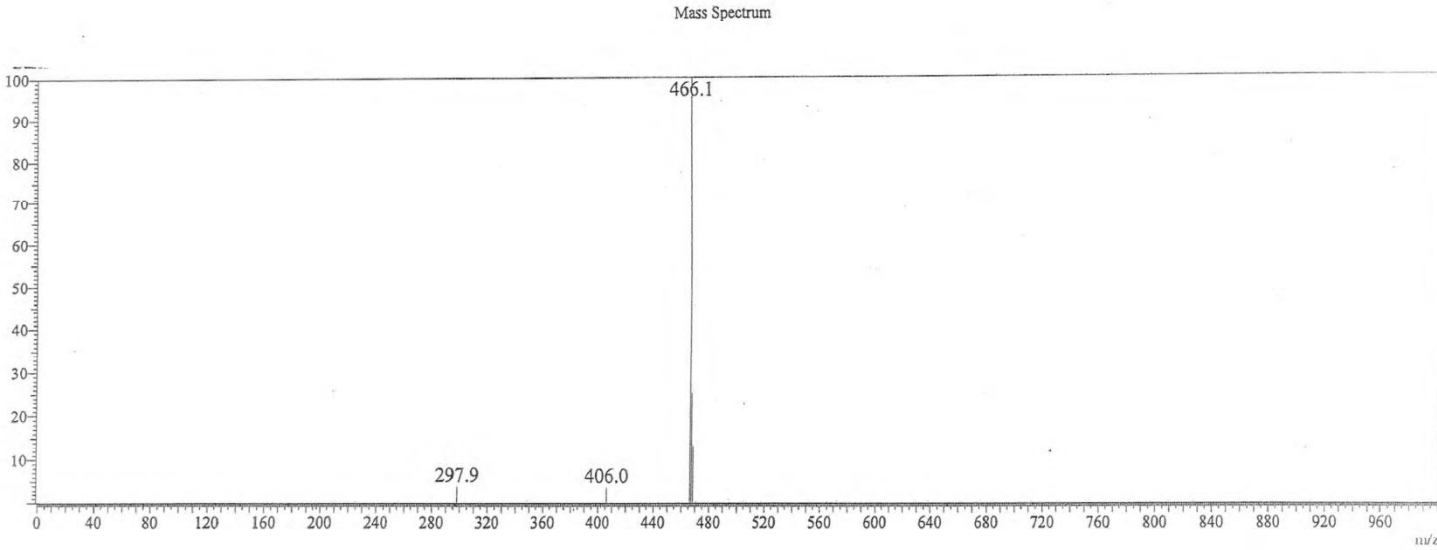
Mass Spectrum
466.1
297.9
406.0
m/z

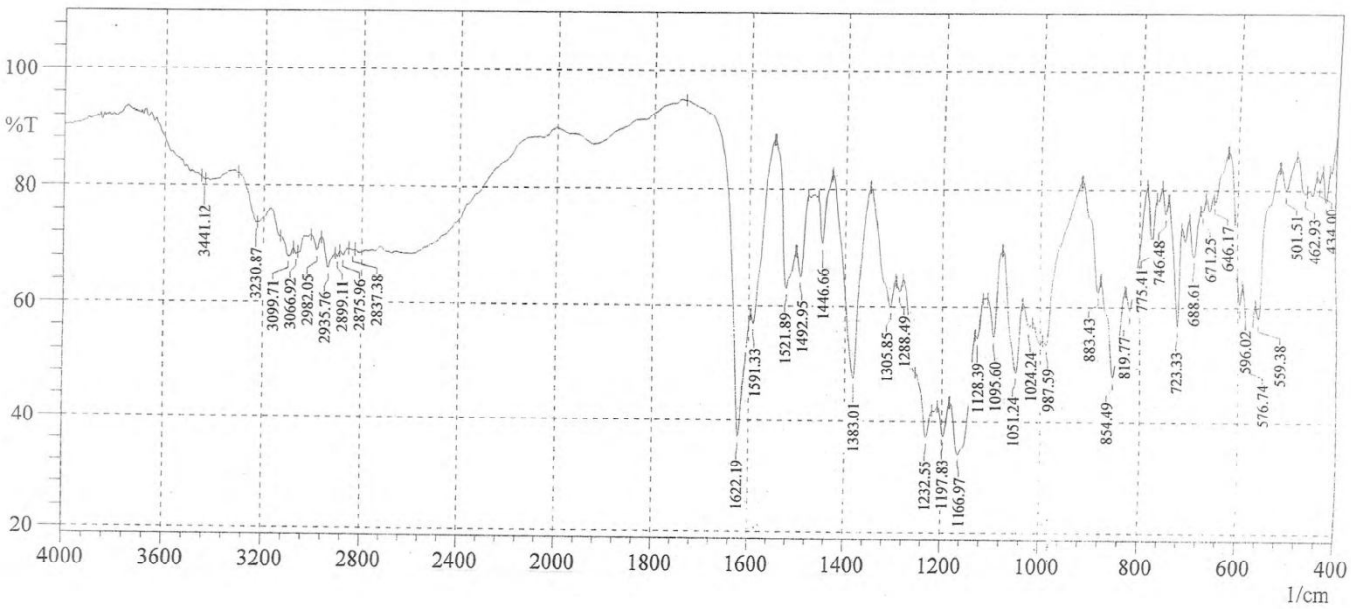
%T
3441.12
3230.87
3099.71
3066.92
2982.05
2935.76
2899.11
2875.96
2837.38
1622.19
1591.33
1521.89
1492.95
1446.66
1383.01
1305.85
1288.49
1232.55
1197.83
1166.97
1128.39
1095.60
1051.24
1024.24
987.59
883.43
854.49
819.77
775.41
746.48
723.33
688.61
671.25
646.17
596.02
576.74
559.38
501.51
462.93
434.00
1/cm

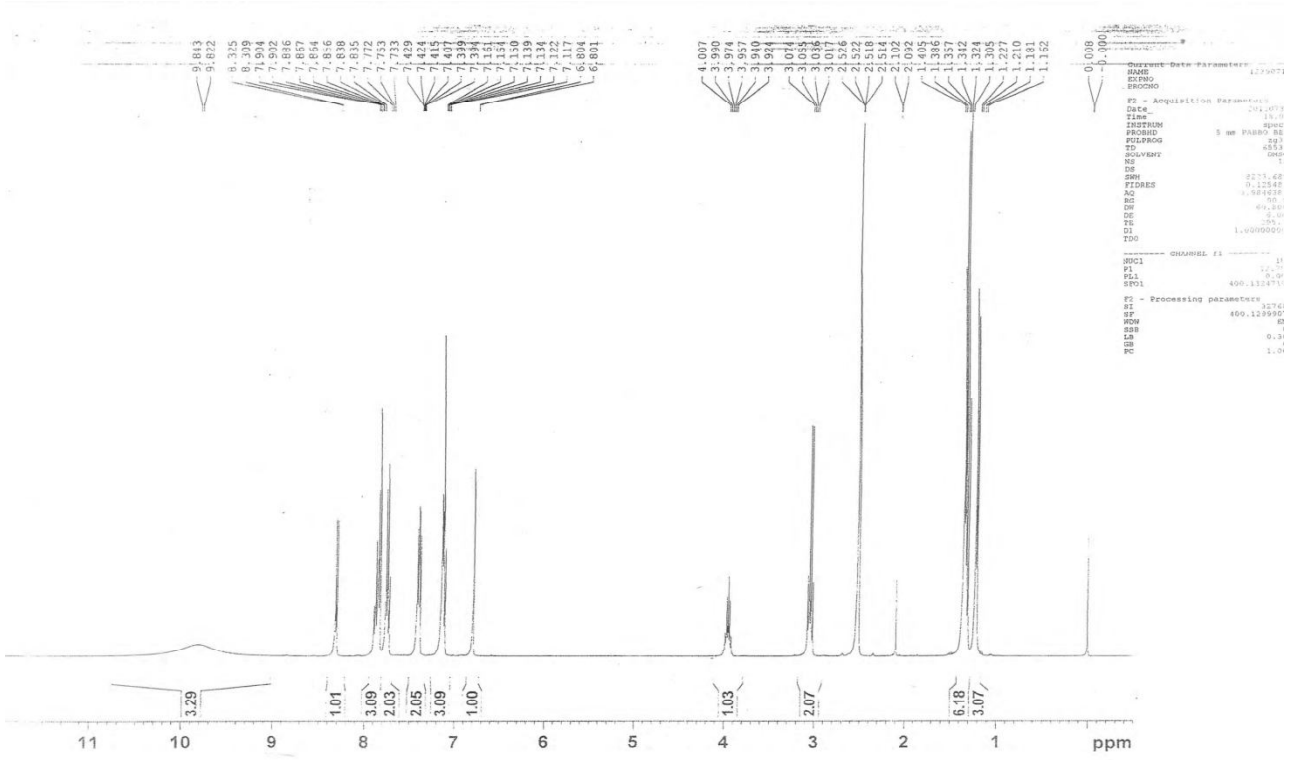
9.813
9.832
8.335
8.319
7.994
7.992
7.886
7.657
7.654
7.636
7.838
7.835
7.772
7.753
7.733
7.429
7.424
7.415
7.407
7.339
7.334
7.151
7.130
7.139
7.134
7.122
7.117
6.804
6.801
4.007
3.990
3.974
3.957
3.940
3.924
3.054
3.038
3.017
2.526
2.522
2.518
2.514
2.102
2.092
1.405
1.386
1.357
1.342
1.324
1.305
1.227
1.210
1.181
1.152
0.008
0.000
3.29
1.01
3.09
2.03
2.05
3.09
1.00
1.03
2.07
6.18
3.07
11
10
9
8
7
6
5
4
3
2
1
ppm

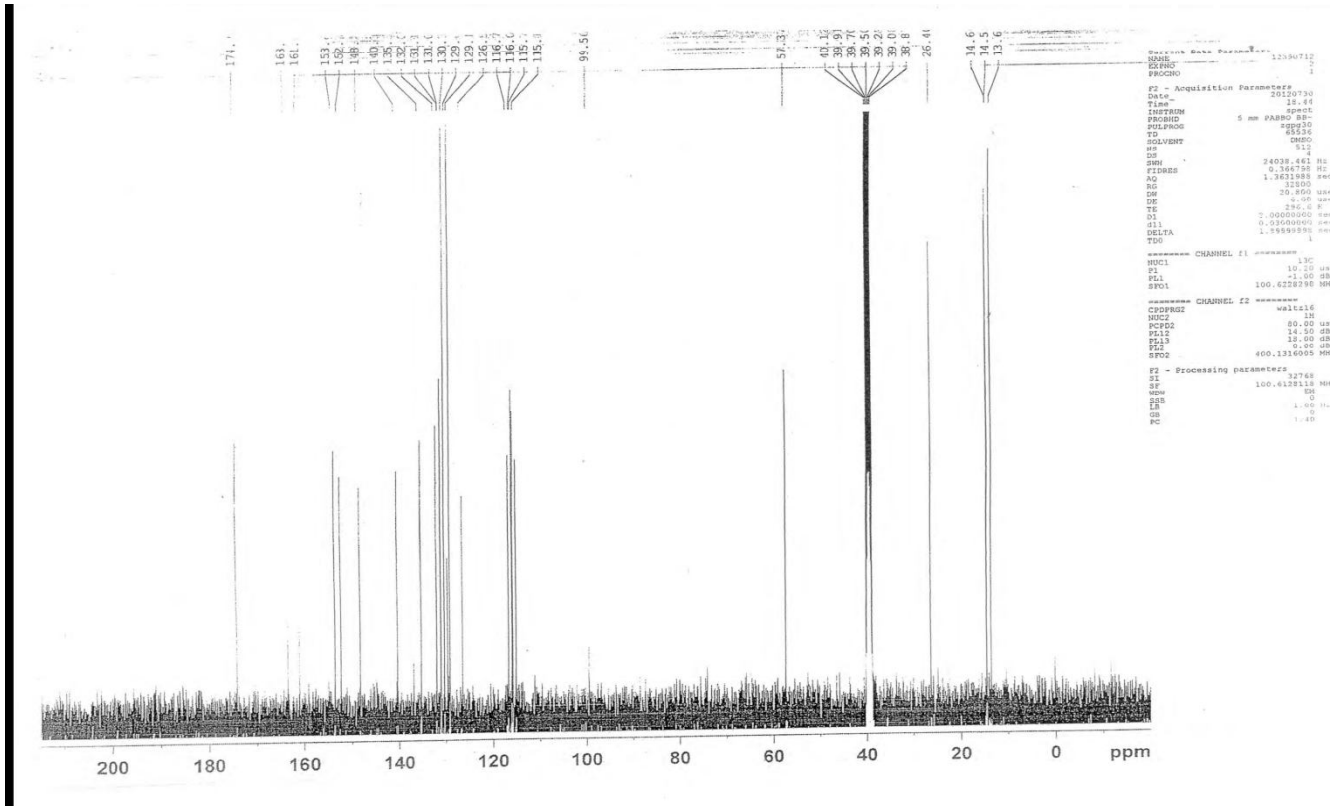
171.
163.
161.
153.
152.
148.
140.
135.
132.
131.
130.
129.
129.
126.
116.
116.
115.
95.5
57.3
40.1
39.9
39.7
39.5
39.2
39.0
38.8
26.4
14.6
14.5
13.6
200
180
160
140
120
100
80
60
40
20
0
ppm

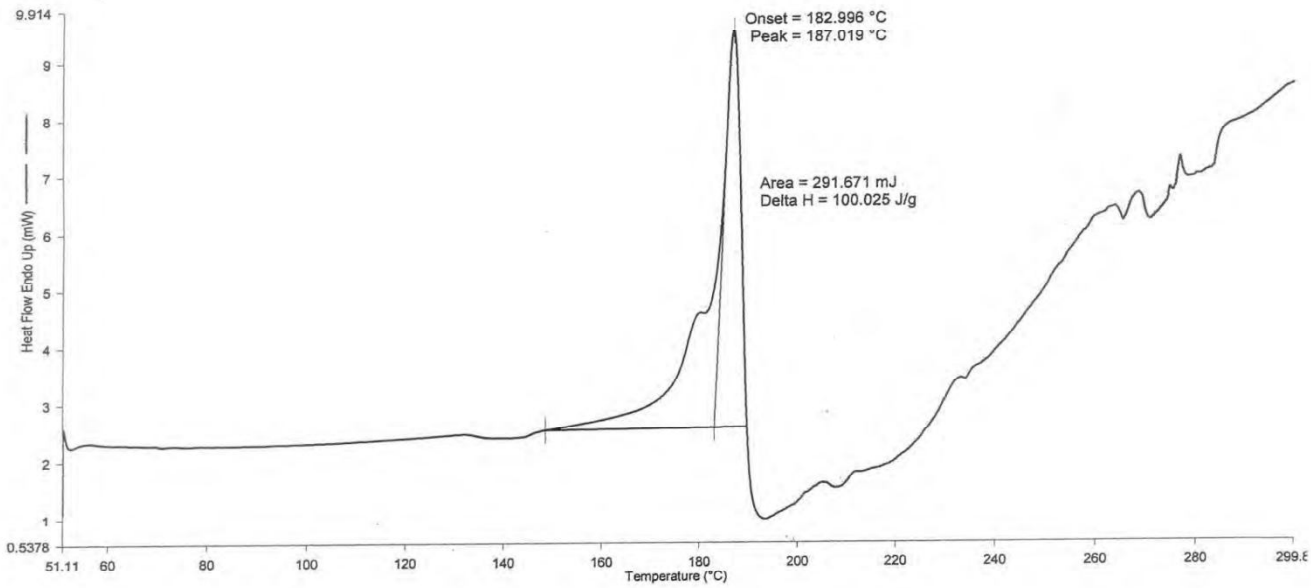
Onset = 182.996 °C
Peak = 187.019 °C
Area = 291.671 mJ
Delta H = 100.025 J/g
Heat Flow Endo Up (mW)
Temperature (°C)
9.914
0.5378
51.11
60
80
100
120
140
160
180
200
220
240
260
280

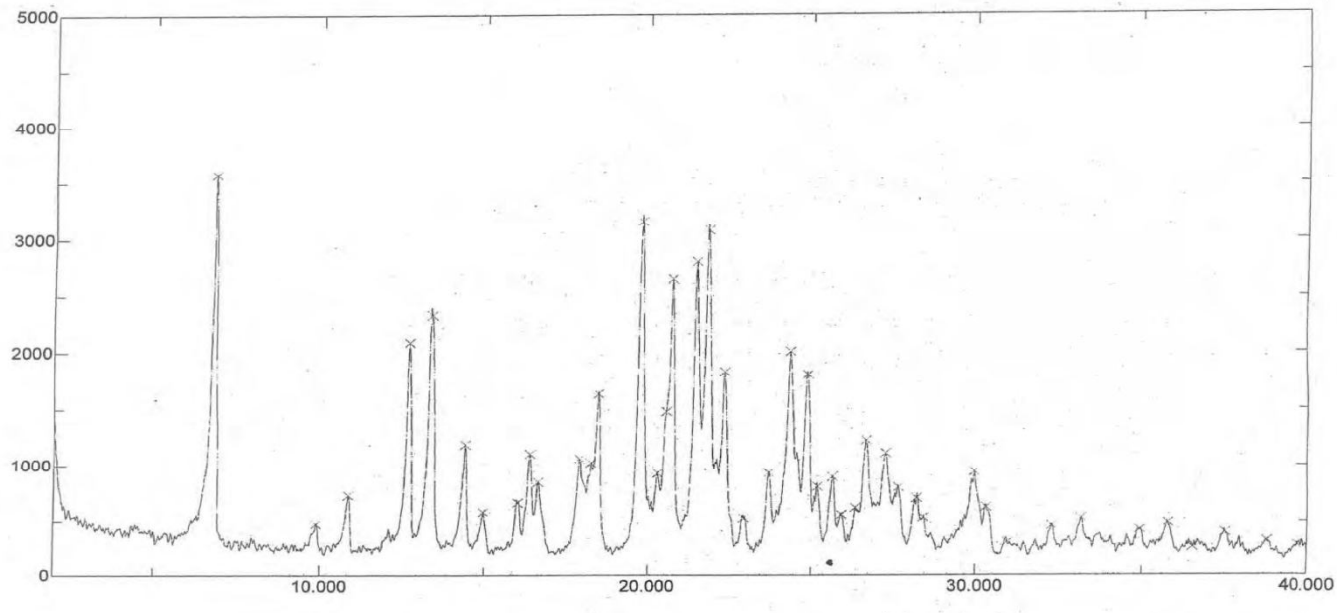
5000
4000
3000
2000
1000
0
10.000
20.000
30.000
40.000

Phosphate salt of compound (1)

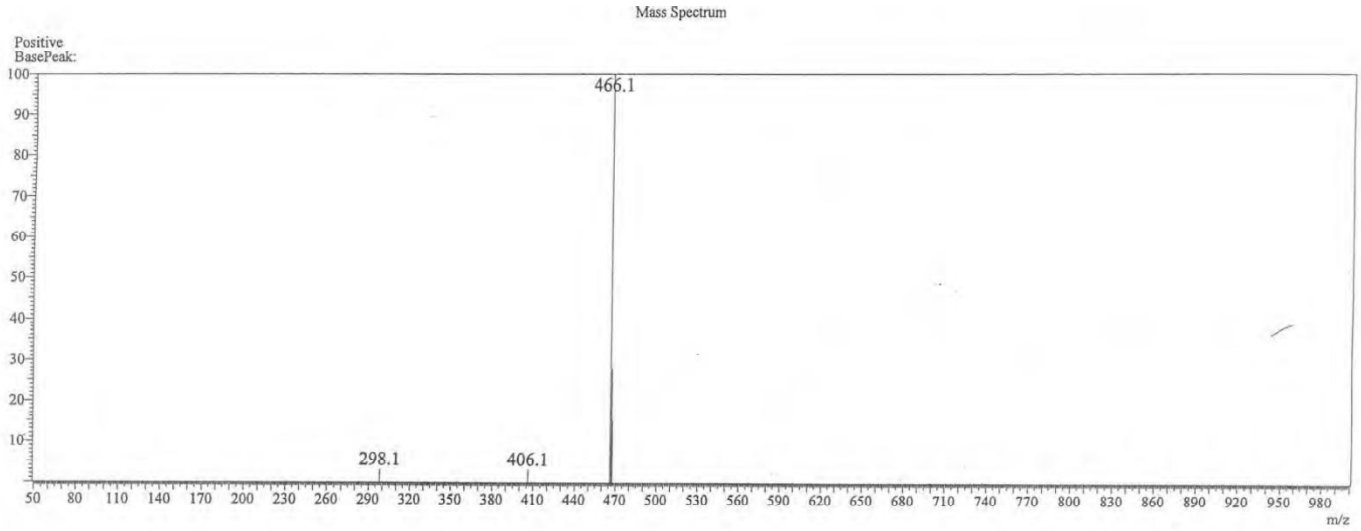
Mass Spectrum
Positive
BasePeak:
466.1
298.1
406.1
m/z

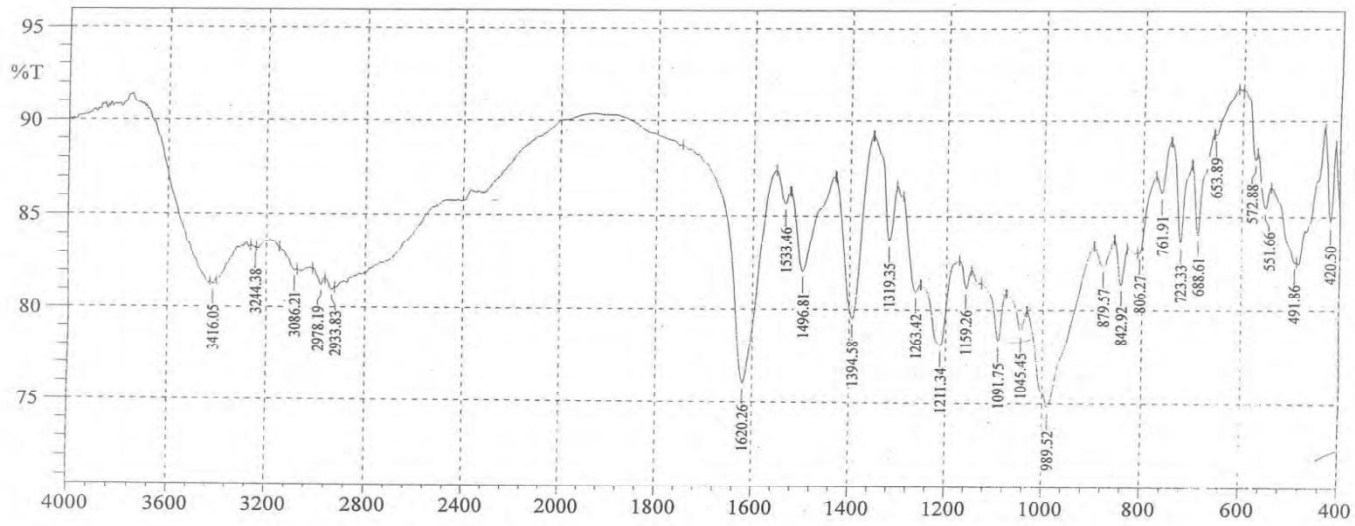
%T
3416.05
3244.38
3086.21
2978.19
2933.83
1620.26
1533.46
1496.81
1394.58
1319.35
1263.42
1211.34
1159.26
1091.75
1045.45
989.52
879.57
842.92
806.27
761.91
723.33
688.61
653.89
572.88
551.66
491.86
420.50

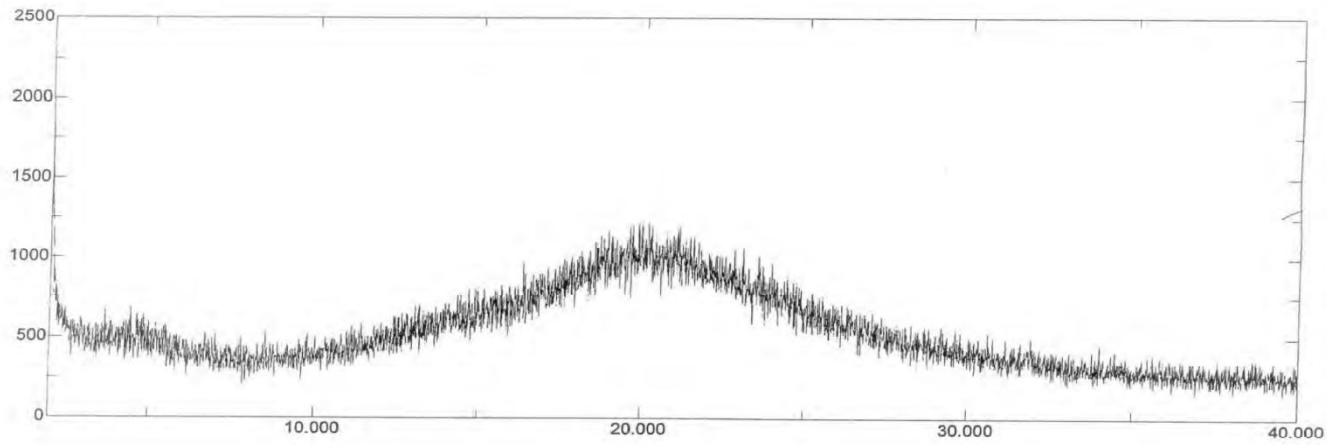
2500
2000
1500
1000
500
0
10.000
20.000
30.000
40.000

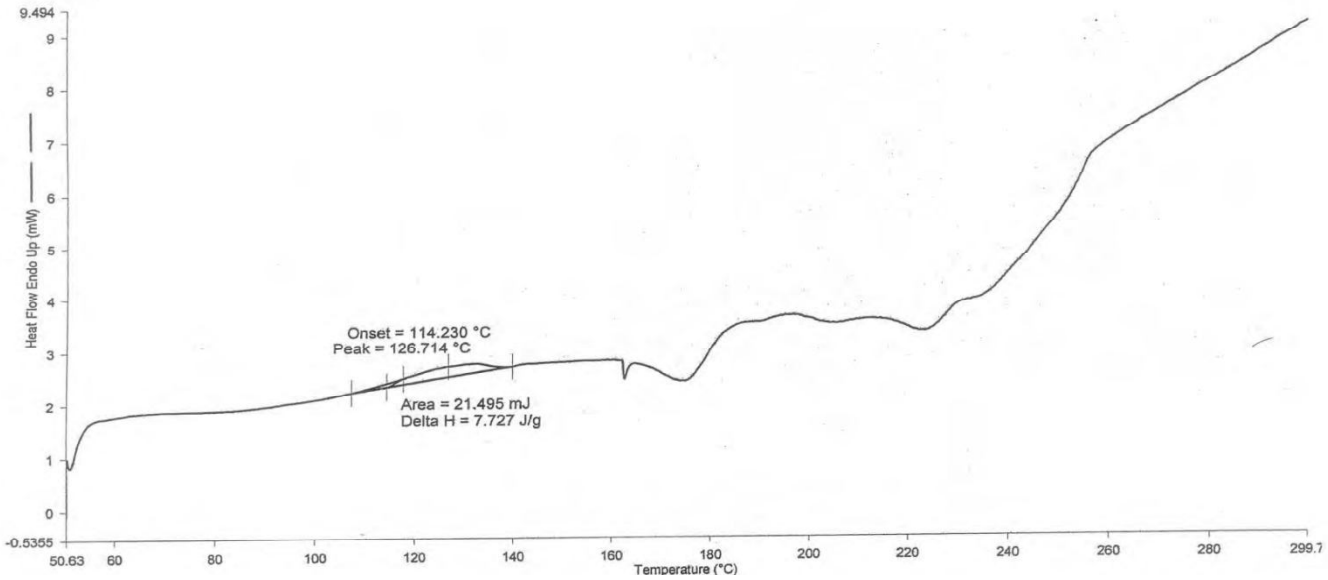
9.494
Heat Flow Endo Up (mW)
Onset = 114.230 °C
Peak = 126.714 °C
Area = 21.495 mJ
Delta H = 7.727 J/g
-0.5355
50.63
60
80
100
120
140
160
180
200
220
240
260
280
299.7
Temperature (°C)

Citrate salt of compound (1)

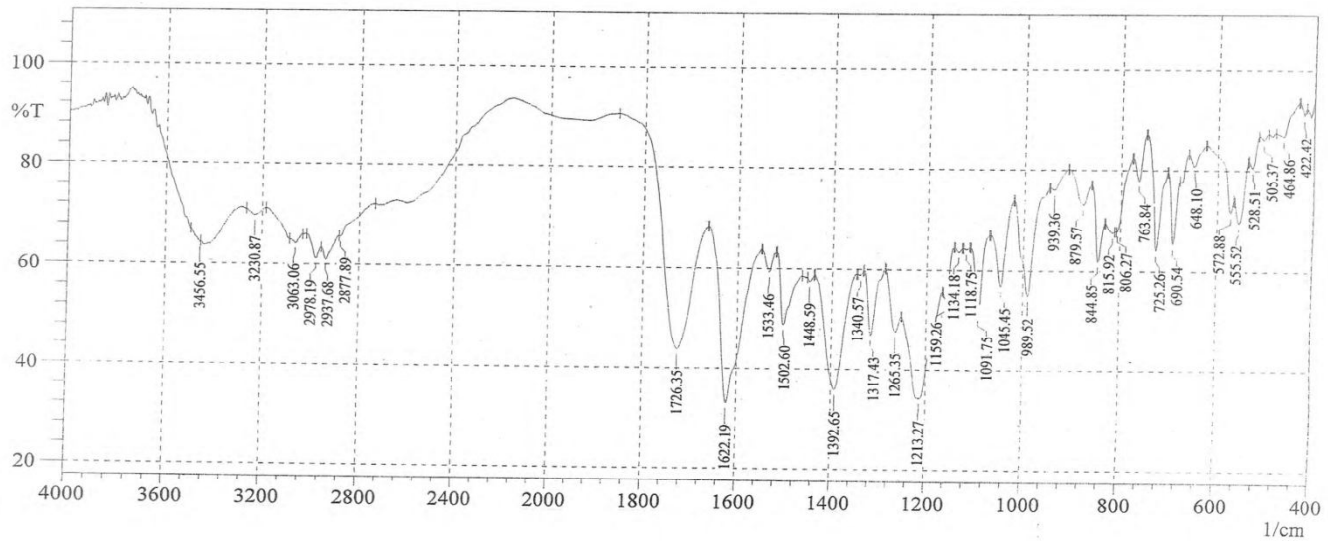

Mass Spectrum

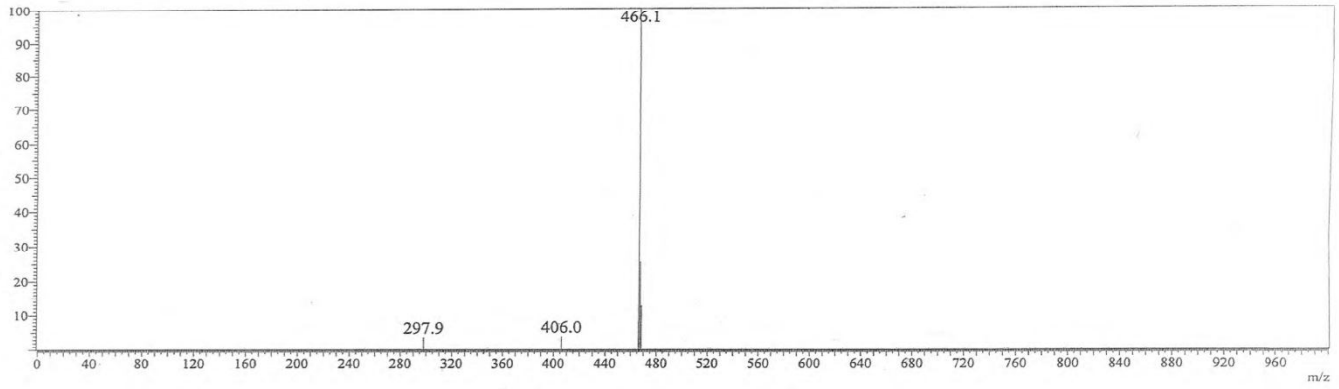

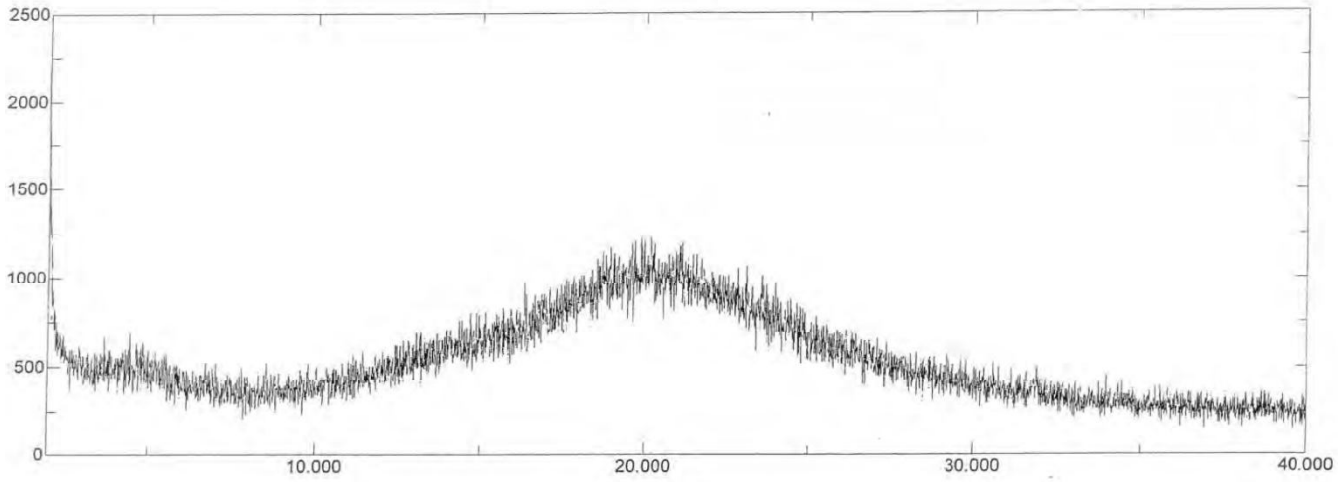
2500
2000
1500
1000
500
0
10.000
20.000
30.000
40.000